Effect of Thickness of ZnSe Thin Films on their Physical Properties

By

Muhammad Imran

Registration No. 46-FBAS/MSPHY/F10

Submitted in partial fulfilment of the requirement for the MS degree
in discipline physics,with specialization in Nanotechnology
at theFaculty of Basic and Applied Science,
International Islamic University,
Islamabad.

Research Supervisor
Dr. Muhammad Mumtaz
Assistant Prof (TTS)

Co-Supervisor
Dr.Aqeel Ahsen Khurram
General Manager, EPL
NCP, Islamabad

June 05, 2012

International Islamic Univ.
CENTRAL LIBRARY
ISLAMABAD.

Accession No TH 9573

MS
530.413
MUE

Physical properties - Zinc Selenide

DATA ENTERED
19/3/13

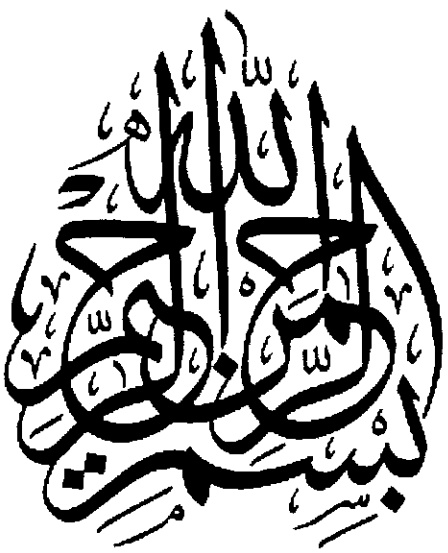

DEDICATED
TO
MY
PARENTS
WIFE
&
DAUGHTER

INTERNATIONAL ISLAMIC UNIVERSITY
FACULTY OF BASIC AND APPLIED SCIENCE
DEPARTMENT OF PHYSICS
ISLAMABAD, PAKISTAN
2012

Effect of Thickness of ZnSe Thin Films on their Physical Properties

By

Muhammad Imran
Registration No. 46-FBAS/MSPHY/F10

A thesis submitted to Department of Physics, International Islamic University for the award of degree of MS physics.

Signature: _____

(Chairman, DOP)

Signature: _____

(Dean FBAS, IIU, Islamabad)

ACCEPTANCE BY THE VIVA VOCE COMMITTEE

Title of Thesis: Effect of Thickness of ZnSe Thin Films on their Physical Properties

Name of Student: Muhammad Imran

Registration No. 46-FBAS/MSPHY/F10

Accepted by the Department of Physics, Faculty of Basic & Applied Sciences, INTERNATIONAL ISLAMIC UNIVERSITY ISLAMABAD, in partial fulfilment of the requirements for the Master of Science in Physics with specialization in Nanotechnology.

VIVA VOCE COMMITTEE

Dean

Chairman/Director/Head

DR. Zulfiqar Hussain Gul Hussain

External Examiner

06/08/12

Research Supervisor

Member

Dated: August 06, 2012

ABSTRACT

Physical properties of ZnSe thin films of various thicknesses deposited in two batches B1 i.e. on In_2O_3:Sn (ITO) coated glass substrate and B2 i.e. on bare glass substrate, by physical vapor deposition, have been studied. X-Ray Diffraction (XRD), Rutherford Backscattering Spectroscopy (RBS), Scanning Electron Microscopy (SEM), Transmission spectroscopy and four probe conductivity techniques were used to characterize the samples. XRD pattern showed that all the films are cubic with preferential orientation along (111). The structural parameters such as grain size D, strain ε, lattice parameters and dislocation density δ are calculated from the XRD patterns. It is observed that the lattice parameters in B1 have shown an increase from 5.678 to 5.834Å with increasing film thickness and become close to that of CdTe which makes ZnSe a suitable window material for CdTe/ZnSe hetero-junction solar cell. RBS analysis shows that indium was diffused into the film from the ITO layer. The optical transmission spectra show that transmission decreases with increasing film thickness and the band gap of samples in B2 are higher than B1 samples. The electrical characterizations show that the films with thickness 71nm and 86nm are more conductive. The sample of B1 series with least film thickness (71nm) has shown highest improvement in conductivity after annealing due to inclusion of ITO and In_2O_3 and might have greater concentration. The samples of B2 were highly resistive but after doping with Ag, their conductivity was improved.

DECLARATION

I ***Muhammad Imran*** (Registration # 46-FBAS/MSPHY/F10), student of MS in Physics (session 2010-2012), hereby declare that the matter printed in the thesis titled "Effect of Thickness of ZnSe Thin Films on their Physical Properties" is my own work and has not been published or submitted as research work or thesis in any form in any other university or institute in Pakistan or abroad.

Dated: June 05,2012.

Signature of Deponent

ACKNOWLEDGMENT

First, I owe my deepest gratitude to Allah Almighty for all of his countless blessings. By virtue of his blessings today I am able to carry out my research work and present it.

I would like to acknowledge the worth mentioning supervision of *Dr Muhammad Mumtaz and Dr Aqeel Ahsan Khurram*. I feel pleasure to mention that Dr. Mumtaz is not only my supervisor but also the person who forced me and convinced me to upgrade my knowledge and encouraged me all the time during my study at IIU Islamabad. I would like to pay special gratitude to Dr. Khurram who guided me and supported me during my whole research work. Also I pay special thanks to Dr. Khurram who provided facilities for RBS at Experimental Physics Lab. NCP Islamabad and guided me to analyze the data, providing facility for annealing and doping the samples at Material science laboratory in EPD, NCP Islamabad. Moreover, their supervision from the preliminary to the concluding level enabled me to develop an understanding of their field. Their wide and deep knowledge have been great value for me.

I would like to offer my special thanks to Dr. Nawazish A. Khan for his guidance during research work and providing me the facility of XRD and conductivity measurement at Material Science Laboratory at Quaid-e-Azam University Islamabad.

I also offer my sincere thanks to Mr. Nasir Mehmood who provided my facility for the preparation of samples and transmission spectroscopy and Mr. Imran for providing SEM facility at NUST Islamabad.

Moreover, I would like to express my sincere thanks to all the faculty members of Department of Physics IIU Islamabad especially to Dr. Waqar Adil Syed (Chairman), Dr. J.I. Saggu, Dr. Kashif Nadeem, Dr Zafar Wazir and Dr. Fakhar e Alam for their valuable suggestions at different stages of my research work. I express my thanks to all staff of Physics Department, IIU, for their various services.

I will express my heartiest thanks to all my class fellows and research colleagues especially Muhammad Shahid, Irfan Qasim, Faisal Jabbar Abbasi, Muhammad Asif Bhatti and Shakib Arslan for being very supportive and co-operative all throughout my research work.

At this time I should remember my friends and colleagues Prof. Tariq Mahmood, Prof. Javed Mahmood and many others for their encouragement, suggestions and valuable help. My sincere thanks are due to My Principal, Head, Department of Physics, and all my worthy colleagues of IMCB, F-10/4, Islamabad for their constant motivation, support and cooperation during the period of my study and research work.

At last but not the least, I am forever indebted to my parents and family members My Mother, Father, Father-in-law, Mother-in-law, sisters, sisters-in-law and my younger brother Muhammad Usman Asad for their prayers, continuous support, love, understanding, endless patience, encouragement and all other possible help throughout the work. Without their help and understanding this work could not have been completed. I feel that this acknowledgement is incomplete without the paying my cordial gratitude to my loving and caring wife who supported and encouraged me a lot during my research work.

Dated: June 05, 2012 ***Muhammad Imran***

TABLE OF CONTENTS

LIST OF TABLES

LIST OF FIGURES

FORWARDING SHEET BY RESEARCH SUPERVISOR

The thesis entitled "Effect of Thickness of ZnSe Thin Films on their Physical Properties" submitted by Muhammad Imran in partial fulfilment of MS degree in Physics has been completed under my guidance and supervision. I am satisfied with the quality of student's research work and allow him to submit this thesis for further process to graduate with Master of Science Degree from Department of Physics, as per IIU rules & regulation.

Date: June 05, 2012.

Muhammad Mumtaz, Ph. D.
Assistant Professor (TTS)
Department of Physics
International Islamic University
Islamabad.

CHAPTER 1

INTRODUCTION AND LITERATURE REVIEW

1.1. SEMICONDUCTORS

On the basis of electrical conductivity materials are classified into three types i.e. conductors, insulators and semiconductors. Semiconductors are those materials whose conductivity lies in between conductors and insulators 10^{3} to 10^{-8} siemen per cm.[1] Semiconductors are insulators at 0K but at room temperatures they show limited conductivity this fact is due to,

- Partially filled conduction band,
- Partially filled valance band,
- A very narrow energy gap between conduction and valance band (~1eV)

Semiconductors can be doped with impurities which alter their electronic properties in a controlled way. There are two types of semiconductors:

- Elemental semiconductors
- Compound semiconductors

1.2. ELEMENTAL SEMICONDUCTORS

In this type of semiconductor, the crystal is composed of atomic elements single type from group IV of the periodic table, the elements of this group includes carbon (C), germanium (Ge), silicon (Si), and tin (Sn). Among these elements

Silicon is the most abundant element on earth as well as the most commonly used electronic semiconductor material.

1.3. COMPOUND SEMICONDUCTORS

In this type of semiconductors, the crystal is formed with the atoms of two or more elements from different groups of periodic table, GaAs, CdTe, ZnSe, GaAsP, AlGaInP etc are some of the examples of compound semiconductors most commonly used. Compound semiconductors are classified into three types;

- Binary (only two elements are present in compound i.e. GaAs, CdTe, ZnSe etc.)
- Ternary (three elements form this type of compound i.e. GaAsP, ZnCdTe etc.)
- Quaternary (four elements form this type of compound i.e. AlGaInP, InGaAsSb etc.)

1.4. Doping of Semiconductors

Doping is a process by which the conductivity of semiconductors can be changed and controlled by adding impurities of some suitable element of periodic table, there are two type of dopant for semiconductors.

- **N-type Dopant or donor impurity:**

For n-type doping of Si, pentavalent impurity (Si is tetravalent) like P or As are added. These atoms are also called donor atoms as they donate a free electron to the semiconductor. Electrons are the majority carriers in this type of doping. In II-VI semiconductors like CdTe, ZnSe, and CdS can be doped n-type by adding any element of group III or VII to these semiconductors.[2] In an n-type semiconductor, due to the higher concentration of electrons than that of holes the Fermi level lies closer to the conduction band.

- **P-type Dopant or acceptor impurity:**

For p-type doping of Si, trivalent impurity like B (boron) or Al are added. These are called acceptor atoms as they accept electrons. Holes are the majority carriers in this type of doping. II-VI compound semiconductors like CdS, CdTe can be doped p-type by adding any elements of group I or V to the semiconductor.[2] In a p-type semiconductor the Fermi level lies closer to the valence band because there is a low concentration of electrons than that of holes.

1.4.1. DIRECT AND INDIRECT BAND GAP SEMICONDUCTORS

Distinguishing characteristic of semiconductors is the situation of the conduction band energy minimum above valance band maximum, on E-k diagram [3]. In Si and Ge, the maximum of valance band does not lie exactly below the minimum of conduction band as shown in Fig. 1.1 (b).

Valance band maximum of all the semiconductors occur at k=0 while the conduction band minimum of Silicon & Germanium (Indirect Band gap) occur at different values of k which indicate a difference of momentum between these two points. In case of GaAs or ZnSe (Direct Band gap) both points, valance band maximum and conduction band minimum, occur at k=0 as shown in Fig 1.1 (a).

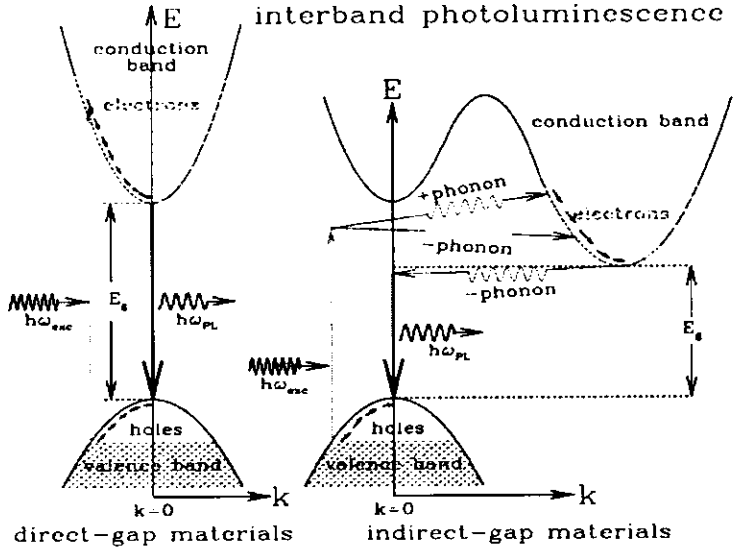

(a) (b)

Figure: 1.1 E-K diagrams of semiconductor band gap (a) Direct and (b) Indirect

In the case of direct band gap semiconductors, a photon of energy hv can excite an electron from the top of the valance band to the bottom of conduction band and an electron in conduction band can fall directly in the hole of valance band by emitting a photon of energy equal to band gap Eg. In case of indirect band gap there is a k- vector shift of conduction band minimum with respect to valance band maximum due to which the electron in conduction band can't fall directly into valance band reason for this is that it have to undergo change in its energy and momentum. Also in case of indirect semiconductor an electron can't excited by a photon from the top of valance band to the bottom of conduction band, because the photon has sufficient energy for this transition but doesn't follow the momentum conservation. An electron motion between the valance band and conduction band of an indirect semiconductor can occur by the action of photon or through a defect in semiconductor, which can provide sufficient momentum for transition. This is the reason due to which direct semiconductors are preferred for optical devices.

1.5. FAMILIES OF SEMICONDUCTORS

The semiconductor crystals are formed by covalent bonding of the conductivity atoms. The bonding electrons lies in the valance band, separated from the conduction band which is completely empty.[4]
There are three families of semiconductors:

- IV-group elemental semiconductors
- III-V compound semiconductors
- II-VI compound semiconductors

1.5.1. IV-group elemental semiconductors

Semiconductors which are composed of only a single atomic element from group IV of the periodic table, semiconductor elements of group IV are carbon (C), germanium (Ge), silicon (Si), and tin (Sn). Silicon is the most abundant and

the most commonly used electronic semiconductor material as shown in Fig. 1.2 (a).

1.5.2. III-V Compound Semiconductors

The III-V semiconductors are formed in such a way that one element is from group III and other from Group V of periodic table. These semiconductors are prominent for applications in optoelectronics. Moreover, III-V semiconductors have ability for higher speed operation than those of silicon semiconductors in electronics applications, particularly their importance in the areas like wireless communications. The crystal lattice of compound semiconductors is constructed from atomic elements in different groups of the periodic table. In this type, compound semiconductors are based in such a way that an atomic element A is from Group III and an atomic element B is from Group V. Each Group III atom is bound to four atom of Group V, and each atom of Group V is bound to four atoms of Group III, general arrangement is as shown in Fig. 1.2 (b). Bonds are formed by sharing of electrons in such a way that the valance band of each atom is filled with 8 electrons. Mainly the bonding is covalent but there is a component of ionic bonding because there is shift of charge from the Group V atoms to the Group III atoms while it is covalent in case of elemental semiconductors. Some of the III-V compound semiconductors are GaAs, GaP, InAs, GaSb, InP, and InSb.

1.5.3. II-VI Compound Semiconductors

II-VI semiconductors are composed with one atomic element from Group II and other atomic element from Group VI and each atom of Group II is bonded to four nearest neighbours of Group VI as shown in Fig. 1.2.(c). In this case the charge transferred from Group VI to Group II atoms is more than that in case of III-V compounds therefore the ionic character is more in this case as compare with that of III-V. These semiconductors can be created in ternary and quaternary forms, much like the III-V semiconductors. II-VI compounds are not much common as the III-V semiconductors, but have some important

applications. Some of the II-VI semiconductors are ZnTe, ZnSe, ZnS, CdS, CdTe and CdSe

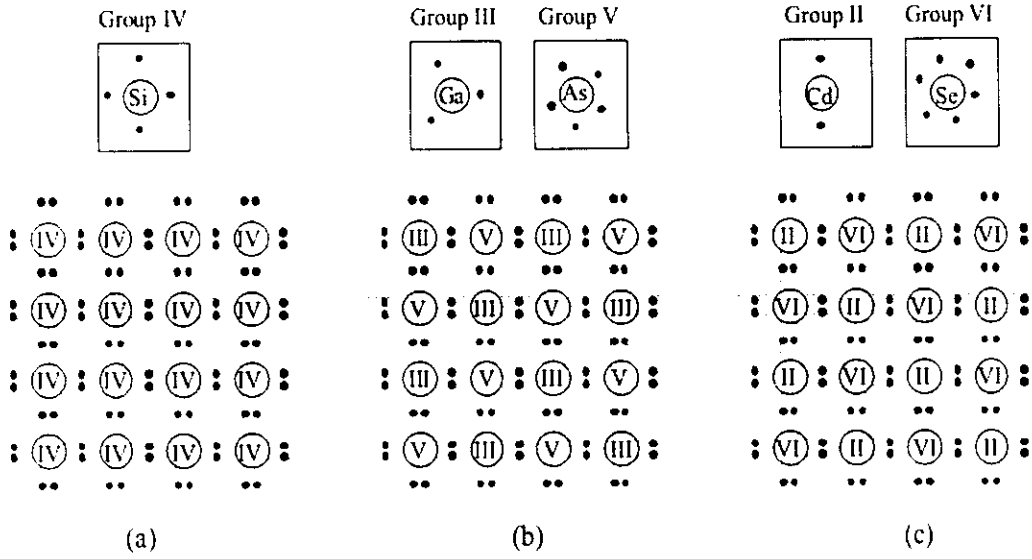

Figure: 1.2. Bonding arrangements of atoms in semiconductor crystals. (a) Elemental semi-conductor such as silicon. (b) Compound III-V semiconductor such as GaAs. (c) Compound II-VI semiconductor such as CdS.

1.6. PROPERTIES OF II-VI COMPUND SEMICONDUCTORS

Before studying the applications of II-VI compound semiconductors, here we will briefly describe some of the structural, optical and electronic properties of II-VI compound semiconductor materials.

1.6.1. STRUCTURAL PROPERTIES

II-VI compound semiconductors are either zinc blende (Cubic) or wurtzite (Hexagonal) in structure, structural lattice of both are shown in Fig. 1.3.(a, b). Among the II-VI semiconductors ZnTe, ZnSe and ZnS are in the form of zinc-blende lattice structure, while CdS and CdSe are either the zinc blende or the wurtzite lattice structure and CdTe forms in the wurtzite lattice structure. In case of Zinc blende structure the lattice constants (in nm) are, ZnS (0.541), ZnSe (0.567), ZnTe (0.610), CdS (0.582), CdSe (0.608) and CdTe (0.648) [5]while in case of Wurtzite structure, the lattice constants a_o and c_o (in nm) are ZnS

(0.3811/0.6234), ZnO(0.32495/0.52069), ZnSe (0.398/0.653), ZnTe (0.427/0.699) CdS (0.4135/0.6749) and CdSe (0.430/0.702).

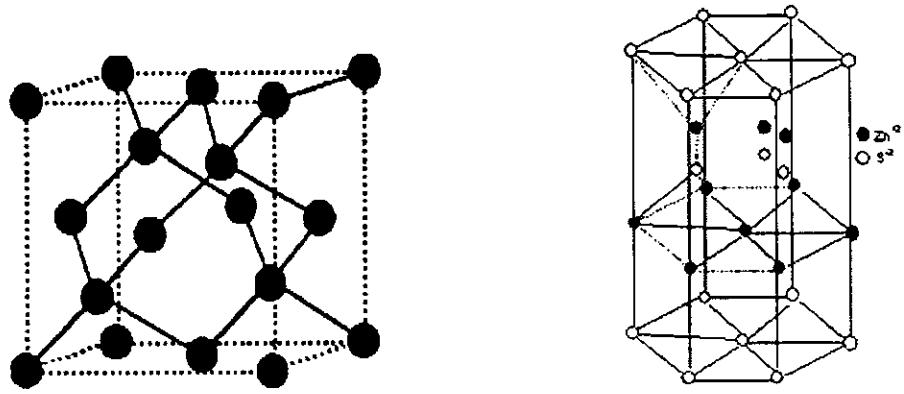

(a) (b)

Figure: 1.3. (a) Zinc blende (Cubic) (b) wurtzite (Hexagonal)

1.6.2. OPTICAL PROPERTIES

II-VI compound semiconductors are direct band gap semiconductors which is a positive feature of these semiconductors over Si as there is no change of momentum take place in case of transition of electron between valance band and conduction band. also these are wide band gap semiconductors their band gaps (in eV) at room temperature are ZnS (3.68), ZnO (3.4), ZnSe (2.71), ZnTe (2.394), CdS (2.5), CdSe (1.75) and CdTe (1.475) and their absorption co-efficient (in cm^{-1}) are ZnS ($\leq$ 0.15), ZnSe ($1\text{-}2x10^{-3}$), CdS ($\leq$ 0.007), CdSe ($\leq$ 0.0015) and CdTe ($\leq$ 0.003).

1.6.3. ELECTRICAL PROPERTIES

Because of wide band gap most of the II-VI compound semiconductors are insulators, by doping them their conductivities can be increased significantly. Elements from group 1B such as Cu, Ag and Au are very important dopants in II-VI compound semiconductors. In addition to their addition as acceptor impurity, they occupy interstitial lattice site to show a high diffusivity at relatively low temperature.[6] ZnSe and CdTe are only II-VI compound semiconductors which can be doped as both n- type and p-type extrinsic semiconductors.[7]

Before going into the details of the applications of II-VI compound semiconductors in the thin film solar cells, we will first describe the basics of solar cells.

1.7. SOLAR CELL

Expected increasing cost of fossil fuels have forced the research to find new resources of energy generation to meet the increasing energy demands of the universe, solar cells or photovoltaic devices got their attention by the researcher as alternate energy resources. A solar cell or a photovoltaic device is a p-n junction semiconductor device that converts light directly into electricity when exposed to light. This phenomenon of conversion of light into electricity is known as photovoltaic effect. As the sun is the only natural source of light for the earth that radiates light with black body spectrum of electromagnetic waves at 6000K. These photovoltaic devices have a vast range of application among different fields of life like calculators, clocks, toys, night bulbs and remote locations that are not connected to the power supply grid station. Also solar cells are the only power source for the space station for communications and other processes.[8] PV devices can also be used to provide large scale power generation like Building Integrated Photovoltaic (BIPV) and centralized Power stations.[9] currently most advanced photovoltaic cells are based on silicon crystalline and polycrystalline form.[10]

1.7.1. PHYSICAL MECANISM OF CONVERSION OF LIGHT INTO ELECTRICITY

The principle of operation of solar cell can be explained as the photons having energy greater than the band gap energy (Eg) of semiconductor are absorbed, as a result of this act electron from the valance band are raised to conduction band and holes are created in the valance band correspondingly. As a result of absorption of photon in the depletion region of pn-junction, generated electron-hole pairs are being separated by the electric field present in the depletion region and make them to flow through the external circuit/load. If the impedance of the load

matches with that of solar cell then the max power is delivered to the load. Schematic diagram of a solar system is shown in Fig. 1.4.

Solar conversion efficiency is given by equation no 1.1.

$$\eta = V_{oc} I_{sc} FF/P \ldots\ldots\ldots 1.1$$

Where:

V_{oc} is open circuit voltage which is voltage generated with infinite load resistance

I_{sc} is short circuit current which is the current generated with zero load resistance

FF is fill factor which is defined as the ratio of the max. power generated by cell divided by $V_{oc}I_{sc}$) and

P is solar power [49]

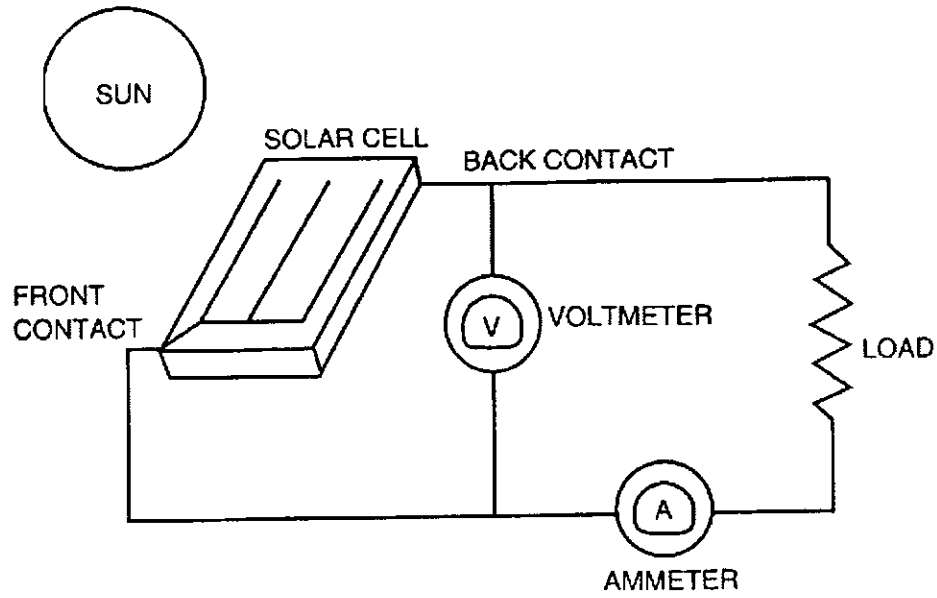

Figure: 1.4. A photovoltaic cell placed in a simple circuit that allows the production of useable power

The researchers have devoted their interest to increase the efficiency of solar cell by introducing new materials for photovoltaic devices. In thin film solar cells the p-n junction is composed of two layers, one is called the window layer and the other is the absorber layer. The function of window layer is to transmit all

the incident photon to the absorber layer, where the electron hole pairs are generated and are collected by the junction potential. The p-n junction is sandwiched between front contact layers which is a transparent conducting oxide with high transparency in the visible region. On the other side of junction another contact layer is formed which could be any suitable metal. Both front and back contacts should be ohmic in nature. Schematic layout diagram of conventional pn-junction thin film solar cell is shown in Fig. 1.5.

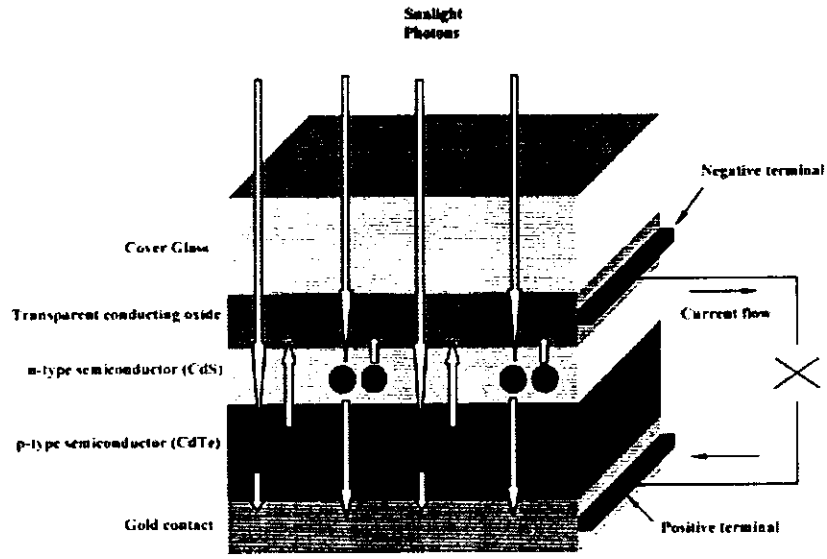

Figure: 1.5. A schematic layout of a conventional pn junction thin-film solar cell.

1.8. APPLICATION OF II-VI COMPUND SEMICONDUCTORS IN THIN FILM SOLAR CELLS

II-VI compound semiconductors are widely used in thin film solar cell as their window layer, absorber layer and buffer layers because of their wide band gap detail of application of different II-VI compound semiconductor, in solar cell, are given as below;

- ZnTe as back contact for CdS/CdTe solar cells [12]
- ZnSe as window layer and buffer layer [13]
- ZnO as front contacts [14]
- ZnS as window layer [15]

- CdS as window layer and buffer layer [16]
- CdTe as absorber layer [17]
- CdSe as window layer [18]

1.9. ABOUT ZnSe

The Zinc Selenide (ZnSe) is a light yellow binary compound (II-VI) semiconductor with a wide band gap of 2.7 eV [19]. The properties such as wide band gap, high photosensitivity and low resistivity make it highly attractive. ZnSe exists in two crystalline forms i.e. zincblende (cubic) and wurtzite (hexagonal), and cubic phase is believed to be stable. At room temperature the ZnSe has the electron affinity of 4.09 eV and electron mobility is about 530 $cm^2 V^{-1}s^{-1}$.[20] Like other II-VI compounds, ZnSe is generally doped as an n-type semiconductor, but is difficult to dope it as a p-type. ZnSe have been doped p-type by using nitrogen as the dopant.[21] Because of direct and large band gap of ZnSe, it has drawn considerable interest among other II-VI compound semiconductors, which makes it appropriate for use in optoelectronics as detectors and emitters. By providing good imaging characteristics, it is useful for optical components in high power laser window and multispectral applications.[22] Its wide transmission wave length range (600 nm to 2000 nm) has made it useful as an IR material.[23] It is used as transmission window in IR spectroscopy, ATR prisms and night vision applications. It is also used in high resolution thermal imaging systems to correct the colour distortion which is often inherent in other lenses used in system. The band gap of ZnSe (2.7eV at room temperature) corresponds to an optical absorption threshold at 460 nm. Therefore the material is useful for the active region in blue-green emission light emitting diodes (LED) [24] and blue diode lasers.[25] Due to high transmission coefficient of ZnSe, it is used as window layer in solar cells. Therefore it can substitute CdS in photovoltaic solar cell devices, which will result in higher cell efficiency by means of admission of more photons to the absorber layer, because of its larger band gap.[26] ZnSe doped with tellurium can be used in ultrasonic transducers. Doped ZnSe is used as host layer of thin film electroluminescent devices.[27] These wide application

possibilities of ZnSe have given considerable importance to the investigation of its thin films in recent years.

1.10. A BRIEF REVIEW OF RESEARCH WORKS ON ZnSe AND THIN FILMS

The optoelectronic semiconducting material ZnSe has been extensively studied as single crystals and also as epitaxial and polycrystalline thin films prepared by different techniques because of its unique optoelectronic and other properties with a hope of exploring potentialities for fabrication of new scientific and technological devices. The inter band electronic property of zincblende ZnSe was theoretically and confirmed them experimentally by Markowski et.al. [28] J. Dutta, et al studied the photoconductivity in poly crystalline semiconductors and grain boundary effect. They showed that the carrier recombination at grain boundaries drastically influence the carrier transport mechanism in layers. This was done theoretically and was confirmed by them experimentally. [29] Effect of thermal annealing on band gap and optical properties of chemical bath deposited ZnSe thin films were studied by F. I. Ezema et.al. They reported that due to change in the morphology as a result of air annealing film showed a red shift of 0.10eV to 0.20eV in optical spectra. [30] Thickness of the film affect the physical properties of thin film, Enriquez and Methew reported the influence of the thickness on structural, optical and electrical properties of chemical bath deposition CdS thin films as the variation of the band gap between conduction and valance band because of straqin of films and in relatively thiner films the trapping centres were less while thicker films were less photosensitive. [31] Lokhande et al studied the deposition and characterization of chemical bath ZnSe thin films and showed that thin films of ZnSe can be deposited by Chemical bath deposition (which is relatively simple and cheap method). These films deposited on various substrate temperatures were found to be amorphous in nature containing oxygen and nitrogen in addition to Zn and Se and they showed that these films are photoactive. [32] Microstructural characterization and optical properties of ZnSe thin films were reported by Rusu et al. that the preferred orientationof ZnSe films by qausi-closed technique is (111) which was confirmed

by XRD and HRTEM. They calculated the band gap as 2.5eV and 2.80eV. [33] Further AFM images showed that the films were homogeneous and of uniform grain size. By heat treatment increased orientation degree of crystalline was observed [34] Chandramohan et al studied the preparation and characterization of semiconducting ZnCdSe thin films. Electrodeposited films of ZnCdSe based on cyclic voltammetry and their wurtzite nature was confirmed by XRD. Also they showed that how the composition of ZnSe and CdSe changes the band gap between 2.82eV and 1.72eV, they also reported their surface morphology was studied by SEM and composition analysis was done by XRD and EDAX [35] Venkatachalam et al reported the composition, structural, dielectric, DC and optical properties of ZnSe thin films deposited by vacuum evaporated, RBS was used to study the composition analysis which was stoichiometric. XRD confirmed their cubic nature also they calculated their grain size D, lattice strain ε, dislocation density δ, and their lattice parameter and they calculated their dielectric constant as 8.11. [36] In another paper Venkatachalam et al reported the properties and characterization of ZnSe films deposited by vacuum evaporated technique at different substrate temperature, they showed their crystalline nature and photo response in the visible range.[37] Doping of semiconductor is the defining property of semiconductors, by this process the conductivity of the semiconductors is controlled. Zulfiqar et al studied the physical properties of ZnSe thin films prepared by two source evaporation and their properties after doping, they studied the optical properties by transmittance spectra and calculated the band gap also they showed that by the doping of Ag in ZnSe thin films their resistivity fell from $\sim 10^9$ Ω-cm to 19.6 Ω-cm. [38] Aqili et al reported the properties of Ag doped ZnTe thin films by an ion exchange process, they reported that there was a reduction to 0.01% of resistivity of doped thin films as compare with those were undoped, they also reported that there was a shift of optical band gap, reduction of transmittance and an increase in refractive index was observed.[39]

1.11. OBJECTIVE OF PRESENT STUDY

As the thickness of the film strongly affect the physical properties of the materials i.e. structural, optical and electrical properties. In my present work we have focused on the effect of thickness on the physical properties of ZnSe thin films deposited by Physical Vapour Deposition technique and the effect of air annealing and Ag doping on the physical properties of these films have been studied. Another objective of the present work was to gain understanding of wide band gap semiconductors for solar cell applications.

CHAPTER 2

EXPERIMENTAL TECHNIQUES

2.1. PREPARATION OF THIN FILMS.

Thin films of ZnSe were deposited on glass substrate by Physical Vapour deposition (PVD) at the rate of 0.2nm per second at 80° substrate temperature the vacuum level was set to ~10^{-6} torr. High purity deposition grade powders (ZnSe 99.9%, ITO 99.5% Manufacturer M/s Balzer) were used for thin film deposition, thickness of the films were controlled using quartz crystal thickness monitor. Two batches of ZnSe thin films were prepared

B1. In first batch ZnSe films were grown over 200nm thick In_2O_3: Sn (ITO) coated glass. Samples are named A, B and C.

B2. In second batch films were deposited directly on glass substrate. Samples are named a, b, c.

2.1.1. ANNEALING

The annealing of semiconductor thin film increases the conductivity and grain size. Therefore, all the samples were annealed in air in furnace at 100°C, 200°C and 300°C for one hour and then they were furnace cooled to room temperature.

2.1.2. Ag DOPING

The as grown B2 were highly resistive. There samples were doped with Ag by Ion exchange process Silver has $4d^{10}5s^{1}$ electronic configuration so that it could make

it p-type ZnSe. Before doping samples were annealed at 300°C to increase the adhesion between film and substrate then a solution of $AgNO_3$ was prepared by mixing 1gram of $AgNO_3$ in 1 litre of distilled water and then the solution was heated up to 60°C and the samples were dipped in the solution for 5 minutes. The samples were then annealed at 350°C for one hour and furnace cooled to room temperature.

2.2. CHARACTERIZATION TECHNIQUES

2.2.1. X-RAY DIFFRACTION (XRD):

X-Ray diffraction is a non destructive technique used to determine structural properties such as lattice parameters (10^{-4}Å), lattice strain, grain size, expitaxy, phase composition, preferred orientation (Laue) order-disorder transformation, thermal expansion, dislocation density, identifying crystalline phases and orientation, , it can also be employed to measure thickness of thin films and multi-layers, to determine atomic arrangement. The XRD technique works on the X-Ray diffraction from crystals explained by W.L. Bragg and W.H. Bragg, known as Bragg's Law;

$$2d\sin\theta = n\lambda \quad \ldots\ldots\ldots\ldots 2.1$$

Where d is interplanner spacing, θ is the angle which the incident beam makes with the crystal plane, n is the order of diffraction and λ is the wavelength of the X-Rays used. The schematic diagram of Bragg's Law is shown in Fig. 2.1.

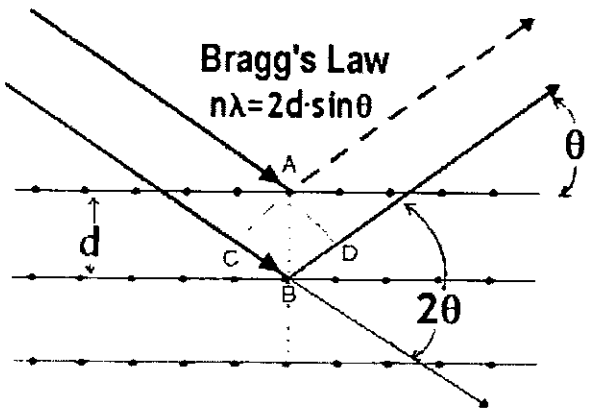

Figure: 2.1 Schematic diagram of Bragg's Law

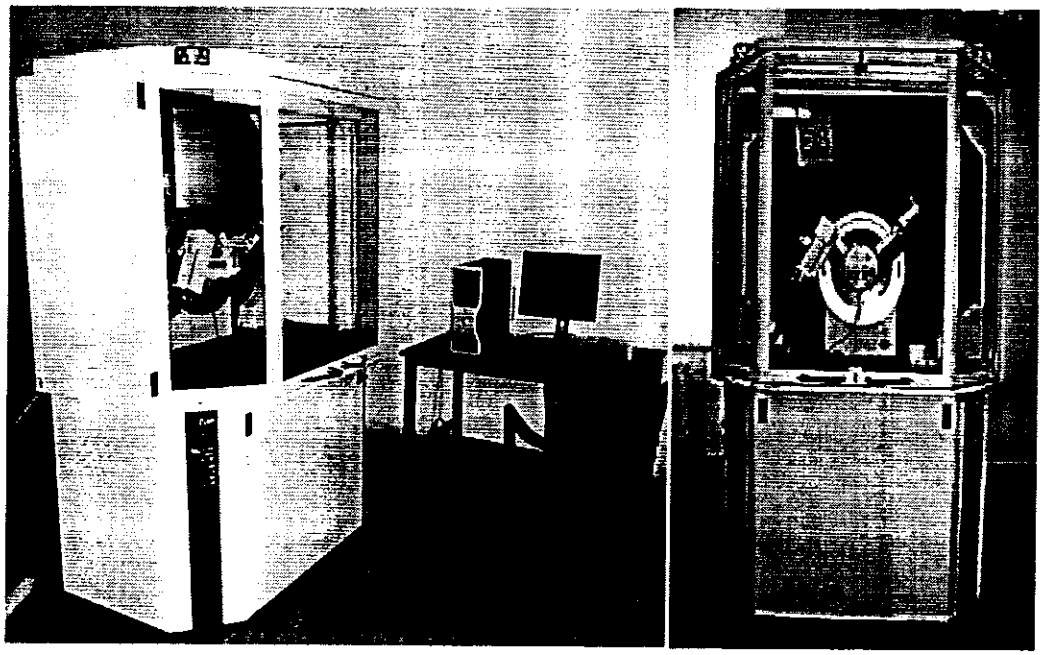

Figure: 2.2 XRD apparatus

In the present work CuKα X-Rays (λ=1.54056Å) have been used to study the crystal structure of ZnSe thin films. The XRD spectra were taken between 2θ~20-80 with scan speed of 1degree per min. The XRD data was taken from X-Ray diffrectrometer D8 Bruker AXS shown in Fig. 2.2.

2.2.2. RUTHERFORD BACK SCATTERING SPECTROSCOPY (RBS)

It is a non-destructive quantitative multi-element compositional analysis technique by which quantitative analysis are possible without using standard reference materials. This technique is named after Lord Earnest Rutherford (a Scientist). This technique was established by Hans Geiger and Ernest Marsden between 1909 and 1914 under the supervision of Rutherford. In this technique an ion like He^{+2} is incident on the sample and due to the interaction with the neuclius of the target atom it is scattered at certain angle if the scattering angle is greater than 90° then it is called backscattering. The energy of back scattered ions are analyezed and compared with the incedent ions as shown in equation 2.2.

$$K = \frac{E}{E_0} = \left[\frac{(M_2^2 - M_1^2 \sin^2\theta)^{1/2} + M_1 \cos\theta}{M_1 + M_2}\right]^2 \quad \ldots\ldots 2.2$$

Where K is kinametic factor E_o is energy of incident ion and E is energy of backscattered ion. M_1 is mass of incident particle and M_2 is mass of target neuclii and θ is the scattering angle.

In the present work He^{++} beam of 2MeV was used at normal incidence and the backscattered beam was detected at Si surface Barrier detector mounted at 10^o relative to the incident beam. The current was set to 20 nA (electrical) to minimize the pile up effect.

Figure 2.3. (a) shows energy of incident ion E_o and energy of backscattered ion E (b) shows block diagram of RBS. Figure 2.4 (a) shows the experimental setup for the study of RBS. A schematic of RBS geometry is shown in Fig. 2.4 (b).

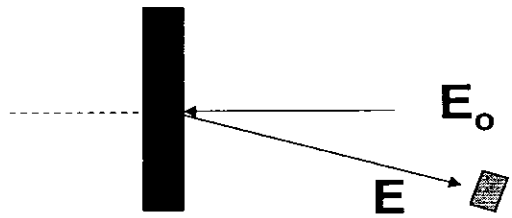

(a)

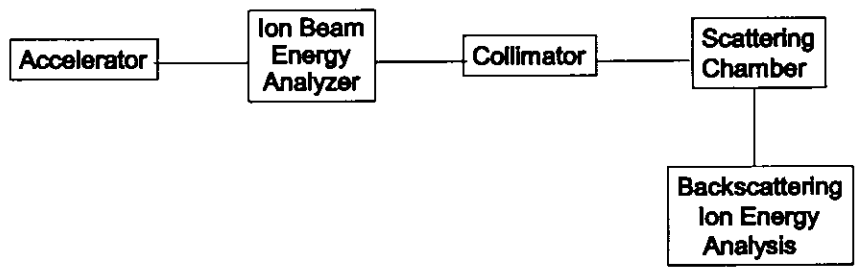

(b)

Figure: 2.3 (a) Ion-target neuclues interaction (b) Block diagram of RBS

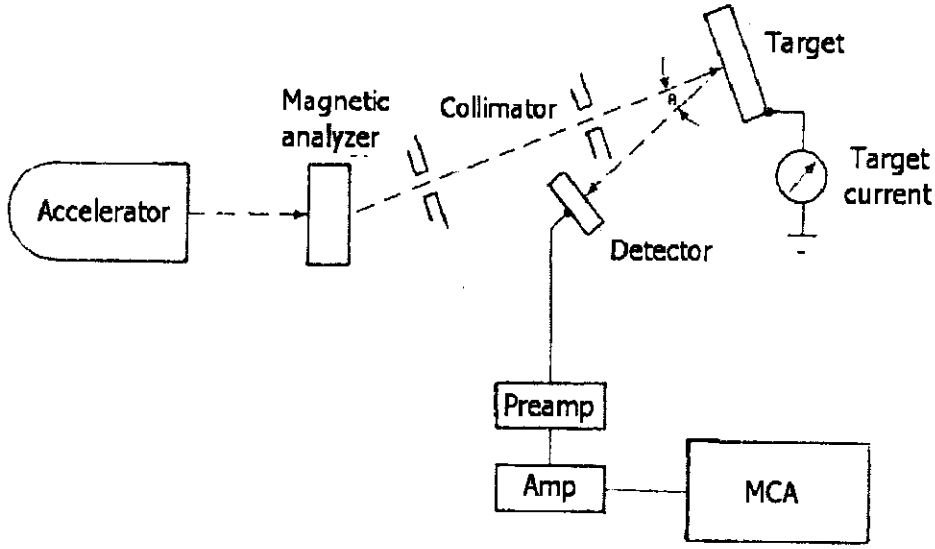

(a)

Figure: 2.4 (a) Experimental set up for RBS (c) Schematic photograph of RBS geometry

2.2.3. TRANSMISSION SPECTROSCOPY

The transmission spectroscopy is a very useful technique to determine the percentage transmission of the optical coatings. The transmission spectrum is alternatively used to measure the absorption edge of the coated material. In this technique a photometer is used which can give electromagnetic waves in near IR, UV and visible region. The electromagnetic radiation fall on the sample some are transmitted, some are reflected and least are absorbed as shown in Fig. 2.5. We have studied the transmission spectra of ZnSe thin films in wavelength range from 200 nm

to 1100 nm using a spectrophotometer perkin elmer lambda -19 uv-vis-nir spectrophotometer. Its working wave lengths are 190 nm to 3200 nm. Abscissa accuracy =±0.15 nm (UV/VIS range), ±0.6nm (NIR range), Ordinate is ± 0.08%T. Detectors used in this apparatus are side window photomultiplier for UV and Visible while PbS detector for NIR. The experimental set up for this apparatus is shown in Fig. 2.6.

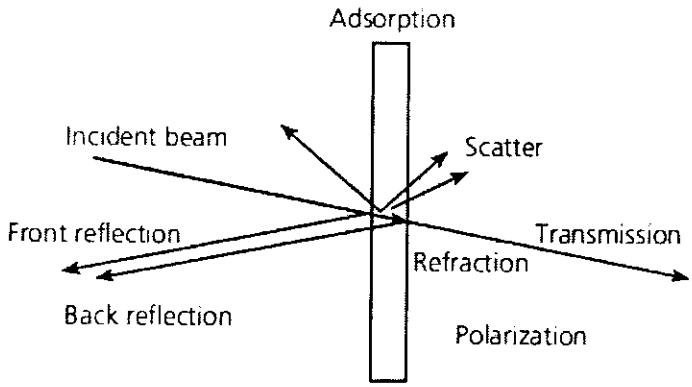

Figure: 2.5 Mechanism of incidence of beam of light on sample

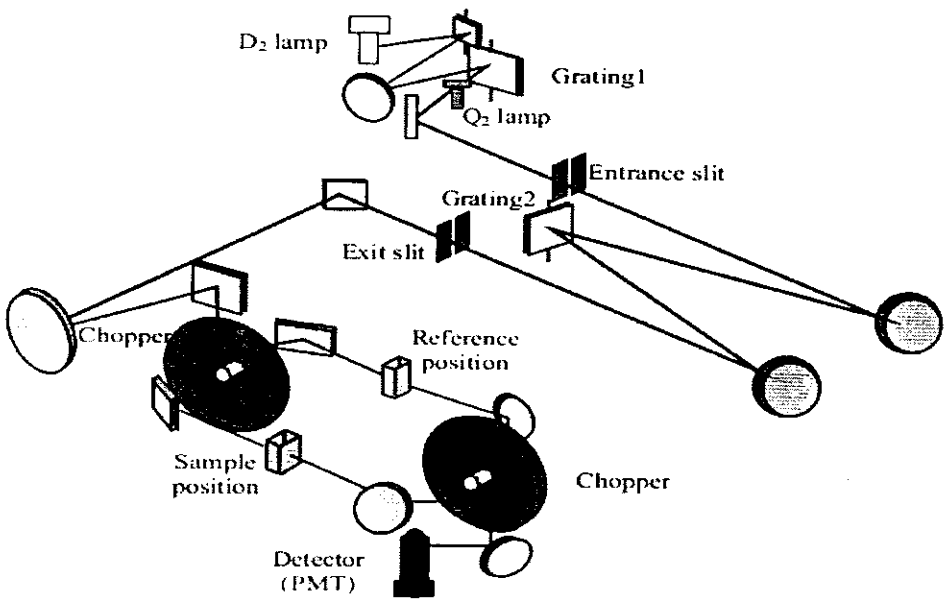

Figure: 2.6 Optical arrangement of spectrophotometer

2.2.4. SCANNING ELECTRON MICROSCOPY (SEM)

The surface morphology of thin film optical coating is very critical from application point of view. The surface smoothness and the grain morphology are studied using SEM. Use of electron microscope was established due to the limiting magnification and resolving power of the optical microscope. In contrast to optical microscope, electron microscope has very large magnification as well as resolving power. The essential components of an electron microscope are electron gun, beam controller and detectors. Schematic diagram of a scanning electron microscope (SEM) is shown in Fig. 2.7.

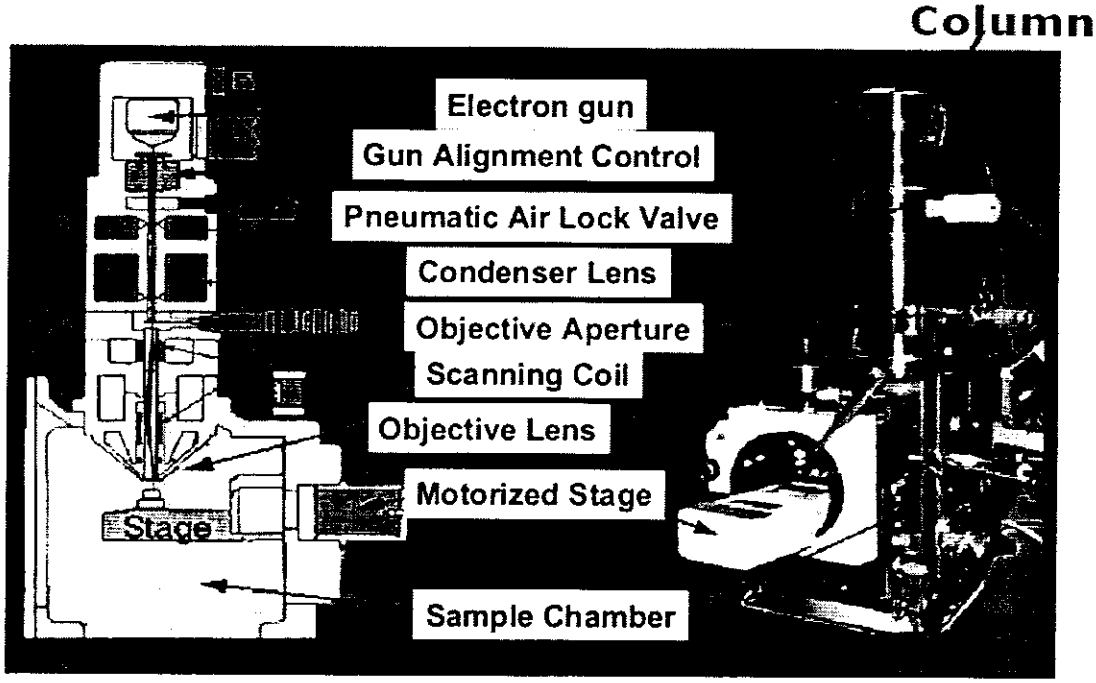

Figure 2.7. Schematic diagram of scanning electron microscope

2.2.5. ELECTRICAL CONDUCTIVITY

Material's surface resistivity can be measured by many ways. two- or four-point probe method is one of the most common methods for measuring surface resistance.[40] In this method either the probes are aligned linearly or in a square pattern to make contact with the surface of the sample.[41] Both methods are the most

common methods for measuring sheet resistivity because they have the ability to minimize the effects of contact resistance Rc.[40,41] The block diagram of two and four point probe methods are shown in Fig. 2.8. In two points probe method a constant Voltage is applied across two points and corresponding current is measured hence I-V characteristics are drawn. The drawback of this method is that in case of materials with high conductivity the resistance of connecting wires also become effective this deficiency can be overcome by using four probes in which constant current is made to flow through material between points 1 and 4 and potential difference between points 2 and 3 is measured by using voltmeter. In the present study four point probe method was used Silver paste was used for the purpose of conducting contacts. I-V characteristics of all the samples were carried out in light and in dark. For light Tungsten Halogen lamp was used. To study the photo decay after the illumination the samples were placed in dark and current decay was recorded for 5min with an interval of 1 minute. The HP 4140 pico ammeter and voltage source has been used to measure the I-V characteristics of the samples. The experimental arrangements used for I-V characteristics in light and dark are shown in Fig. 2.9 (a) and (b) respectively.

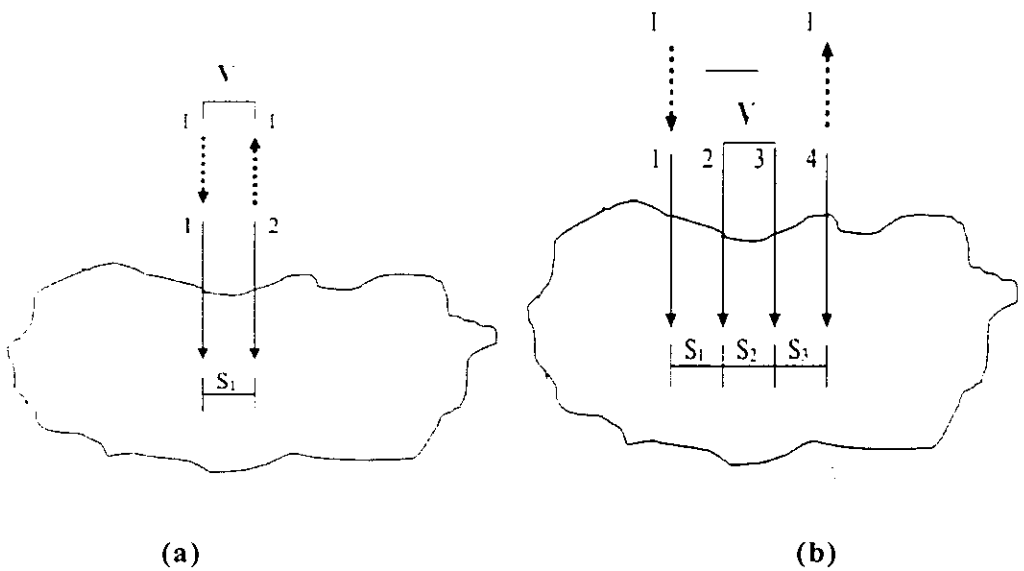

Figure 2.8. Method for resistivity measurement (a) Two Probe, (b) Four Probe

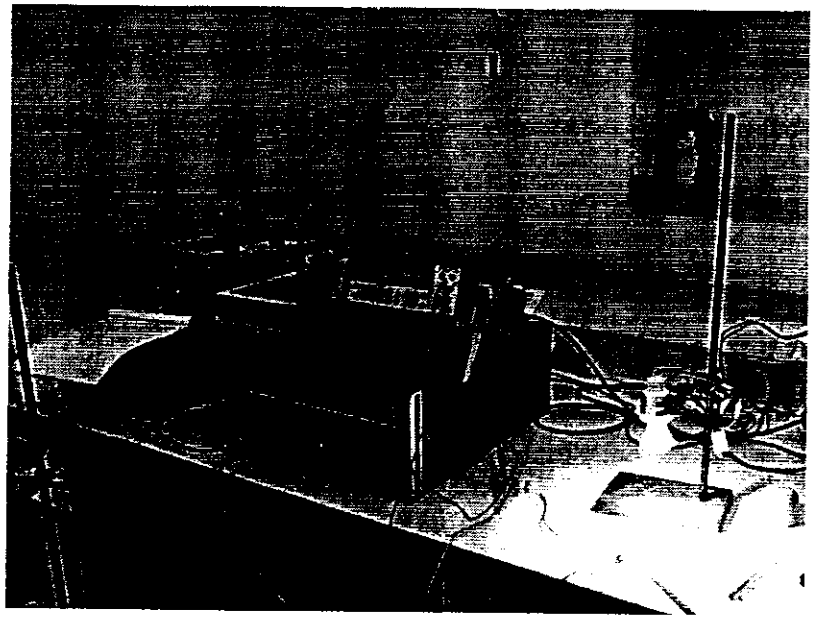

(a)

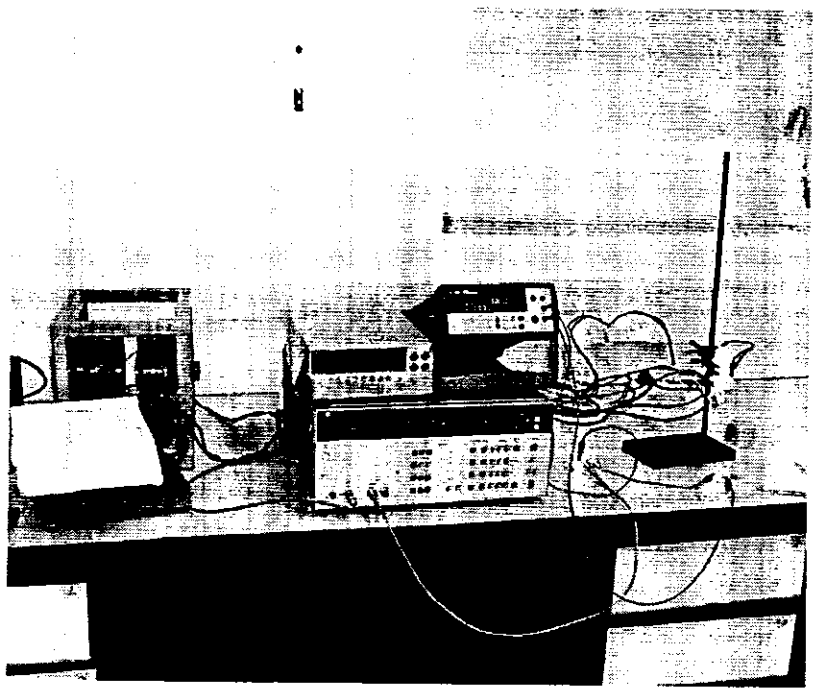

(b)

Figure 2.9. Experimental arrangement for I-V characteristics in (a) light (b) dark

CHAPTER 3

RESULTS AND DISSCUSSION

3.0. INTRODUCTION

Structural, optical and electrical properties of the samples prepared in Batch 1 and 2 have been disused in this chapter. All these properties have been studied in three sections;

- Section-1, properties of as-prepared samples of ZnSe/ITO has been discussed.
- Section-2, properties of samples of B-1 annealed at 100, 200 and 300°C has been discussed.
- Section-3, properties of Ag doped ZnSe have been discussed.

3.1. SECTION-1

In this section the analysis of as prepared samples A, B and C have been described. First of all the results of XRD, RBS and SEM have been discussed for structural characterization then the results of transmission spectroscopy for optical characterization are described in last results of electrical properties i.e. I-V characteristics, Photocurrent and Photo decay and photosensitivity have been discussed.

3.1.1. STRUCTURAL CHARACTERIZATION

3.1.1.1. X-RAY DIFFRACTION

The XRD spectra of ZnSe/ITO/glass thin films (t~71, 77, 86nm) are shown in Fig.3.1 (a-c). The samples with t~70, 77, 86nm will be designated by the alphabets A, B and C respectively in the text. The XRD spectra of ZnSe thin films has shown a cubic structure with preferred (111) orientation observed at 2θ~27.22. However, there is a shift in the (111) peak position to lower 2θ values with the increase in the thickness of the ZnSe films. The crystalline quality has been also improved with the increase of ZnSe thin film thickness. The structural parameters of ZnSe thin film samples were calculated using the (111) peak which are shown in Table 1. It can be seen from this table that the cell parameters have been increased to 5.83 and 5.834Å with the increase in the film thickness. Moreover, no impurity peak was observed from the ITO itself. The values of the cell parameters for the sample A were found to be 5.678Å comparable to the already reported values for ZnSe. [37] The grain size, lattice strain and dislocation density of sample A, B and C were also calculated from the XRD data using equations 3.1, 3.2 and 3.3 respectively. [36]

$$D=0.94/\beta\text{Cos}\theta \qquad 3.1$$

$$\varepsilon=\beta\text{Cos}\theta/4 \qquad 3.2$$

$$\delta=15\varepsilon/aD \qquad 3.3$$

It can be seen from this table that as the thickness is increased there is a decrease in the grain size, whereas the lattice strain and dislocation density has been increased.

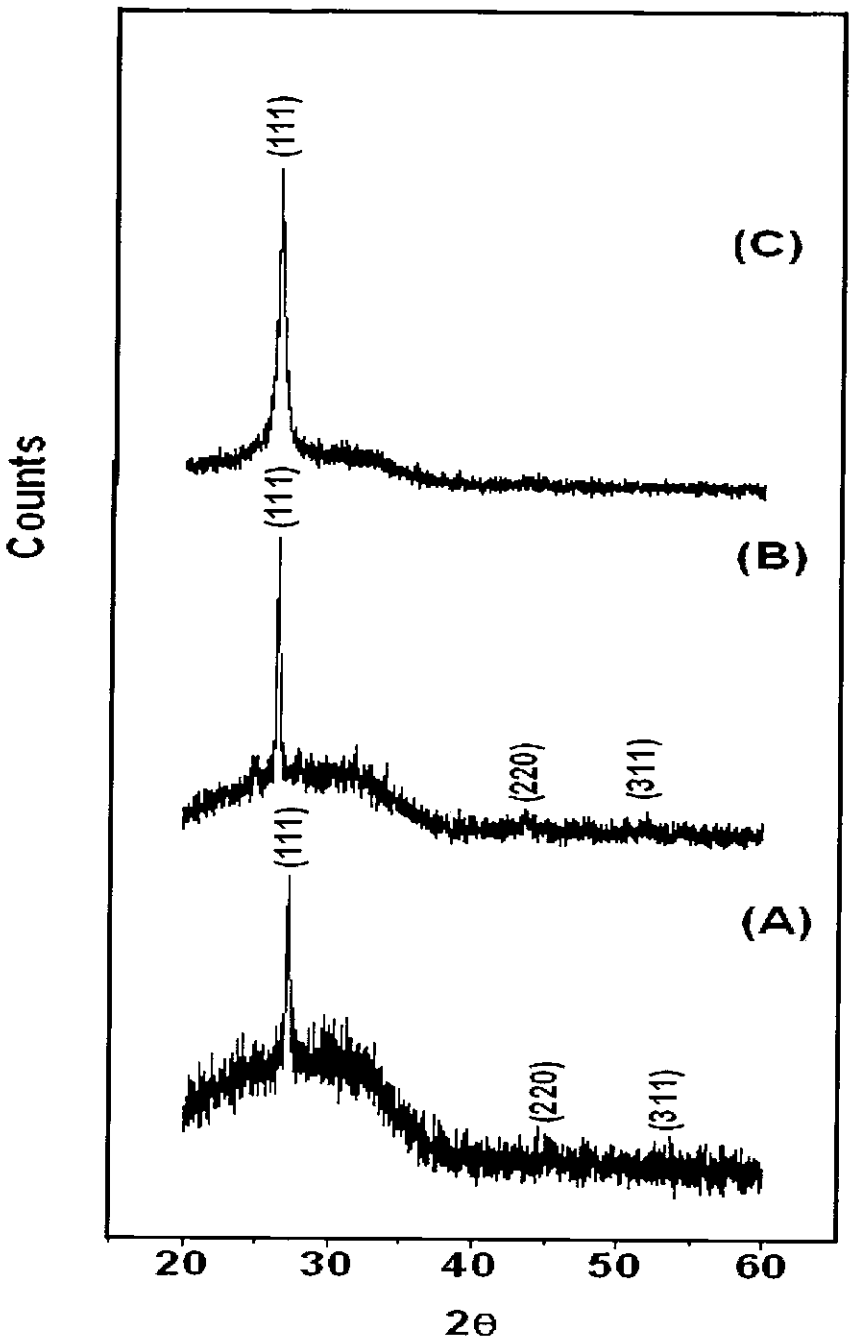

Figure: 3.1 XRD patterns of samples A, B and C.

Sample	2θ	$D = \frac{0.94\lambda}{\beta Cos\,\theta}$	$\varepsilon = \frac{\beta Cos\,\theta}{4}$	$d = \frac{\lambda}{2Sin\theta}$	$a = d\sqrt{h^2 + k^2 + l^2}$	$\delta = \frac{15\varepsilon}{aD}$
	degree	nm	$10^{4}lin^{-2}m^{-4}$	Å	Å	$10^{14}linm^{-2}$
A	27.192	33.89	10.687	3.278	5.678	8.331
B	26.465	33.18	10.703	3.366	5.83	8.299
C	26.45	17.76	20.387	3.368	5.834	29.514
C-300	26.44	42.63	8.495	3.369	5.835	5.123
c	27.2	32.84	11.026	3.277	5.676	8.873

Table 3.1 : Structural parameters of sample A,B, C, C-annealed at 300°C and c on the basis of XRD data, where D is grain size, ε is lattice strains, d is interplanner spacing, a is lattice parameter and δ is dislocation density

3.1.2. COMPOSITION, THICKNESS AND MICROSTRUCTURE:

The composition and thickness of as deposited thin films of B 1 were determined through Rutherford Backscattering Spectroscopy (RBS). The RBS spectra of sample A, B and C are shown in Fig. 3.2. The simulation codes RUMP and SIMNRA were used to calculate the thickness and composition of these samples. The thickness of sample A, B and C are calculated to be 71nm, 77nm and 86nm. Compositional analysis shows that Zn to Se ratio is ~1.12 in all the samples with a significant inclusion of indium from under layer in sample B and C. The Indium might have been introduced during the deposition of ZnSe on In_2O_3:Sn (ITO) film due to very high temperature of ZnSe vapours. The thickness of ITO layer was also determined and found to be 1414, 1770, 1322nm of sample A, B and C respectively. These results have shown that indium (or tin) have been diffused into the ZnSe layer, and probably have occupied Zn or Se sites which have changed the lattice parameter but did not affect the phase purity of the material. The results extracted from RBS analysis are given in Table 3.2.

The microstructure of the ZnSe thin films was studied through scanning electron microscopy (SEM). Two samples were selected for this purpose; one with least thickness and second with largest thickness. The SEM micrographs are shown in Fig. 3.3. It can be seen from these images that there is full coverage of the glass substrate by the film with SEM selected resolution with small amount of clusters on the film surface.

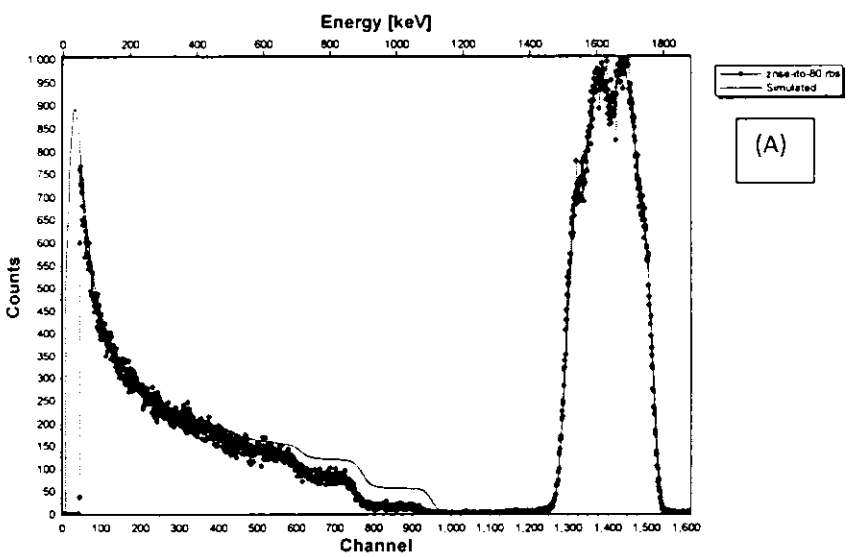

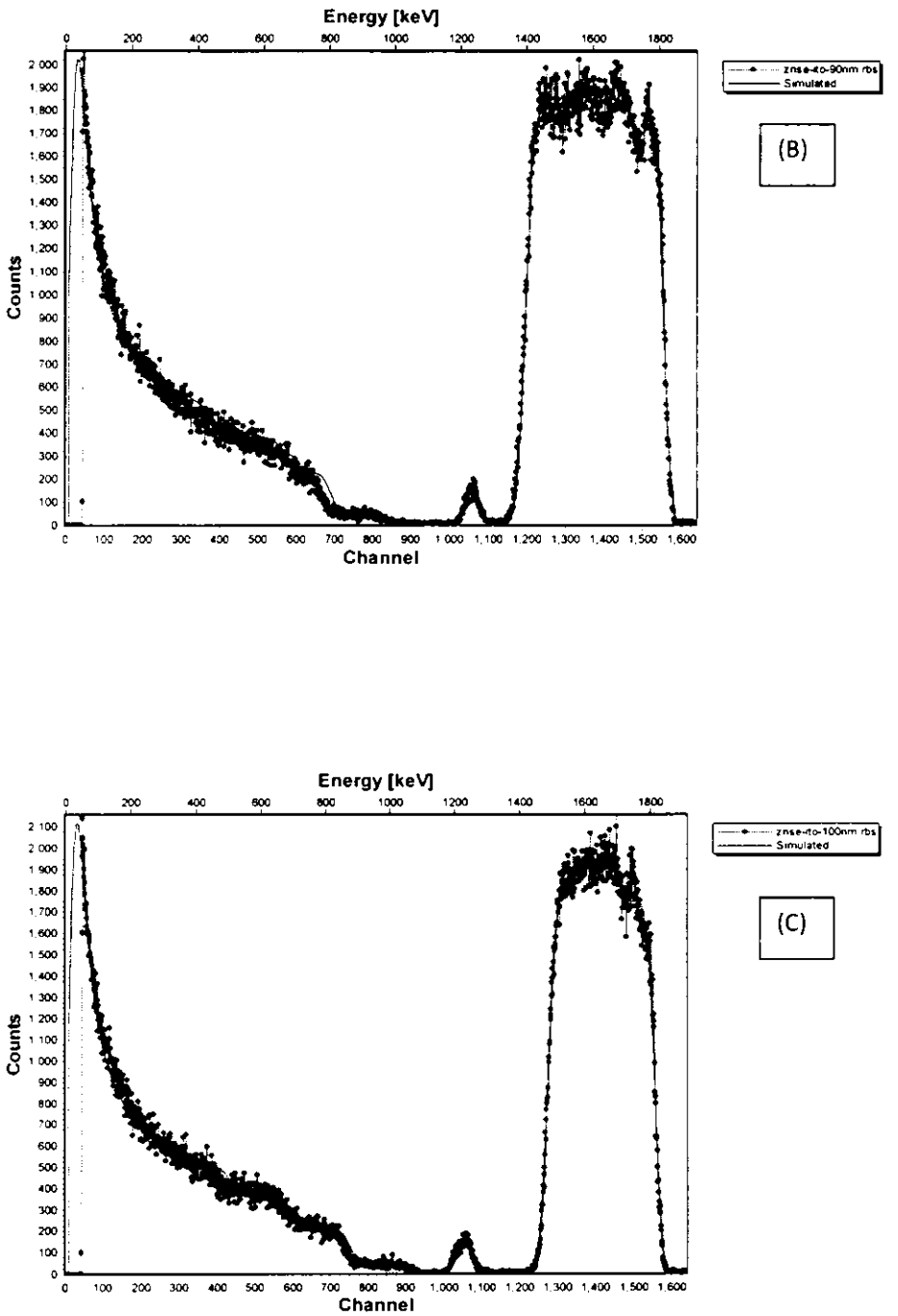

TH 9578

Figure: 3.2 RBS and simulated spectra of ZnSe/ITO thin film samples (a) A, (b) B (c) C

Sample	A				B				C			
Layer 1	t(nm)	Zn%	Se%	-	t(nm)	Zn%	Se %	In %	t(nm)	Zn%	Se%	In%
	71	52.8	47.2	-	77	19	18	63	86	20.4	18.1	61.5
Layer 2	t(nm)	In%	Sn%	O%	t(nm)	In%	Sn%	O%	t(nm)	In%	Sn%	O%
	1414	23.7	22.6	53.7	1770	34.9	7.9	57.2	1322	34.1	7.9	58

Table: 3.2. Results of RBS analysis using SIMNRA

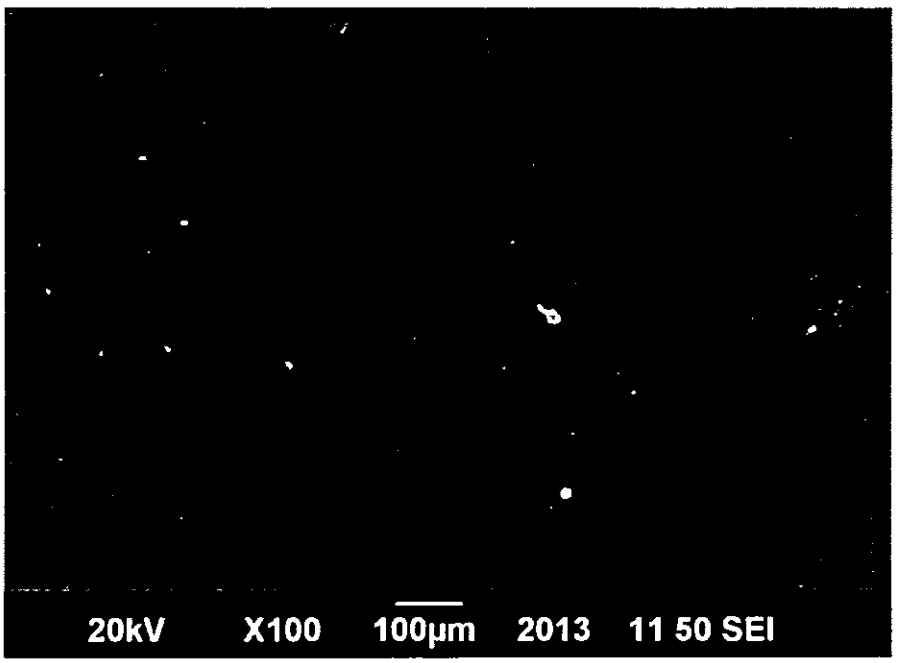

(a)

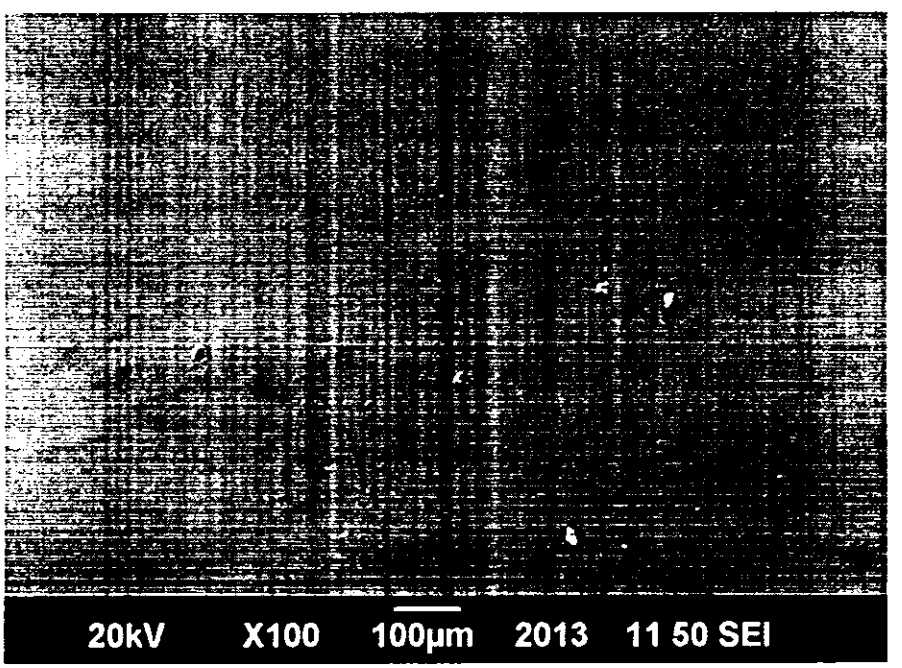

(b)

Figure: 3.3 SEM micrograph of samples (a) A and (b) C.

3.1.3. OPTICAL ANALYSIS

The transmission spectra of A, B and C samples in the wavelength range 200-1200nm are shown in Fig. 3.4. It can be seen from this figure that the samples A and C have shown higher transmission as compared to the sample B. The one possible reason of low transmission of sample B is higher thickness of ITO layer. The absorption coefficient α (cm^{-1}) was calculated using equation 3.4.

$$\alpha=1/[d*\ln(1/T)] \quad \ldots\ldots\ldots\ldots\ldots 3.4$$

Where

d: film thickness

T: Transmission

The effects of reflection and transmission losses in glass and ITO layer were ignored. The absorption coefficients as a function of incident photon energy are shown in Fig. 3.5. It can be seen from this figure that the absorption coefficient is higher in sample B and least in sample C.

The energy gap E_g of the films was calculated from $(\alpha h\nu)^2$ vs hν plots as shown in Fig. 3.6. by assuming direct band gap material. Intercepts were drawn from the linear portion of the $(\alpha h\nu)^2$ vs hν curves. The x-intercepts values are selected as the energy gap of each sample. The calculated band gap values are 2.43, 2.2 and 2.6eV for samples A, B and C respectively. There are various factors which can influence the band gap energy i.e. lattice parameter, grain size, impurities, lattice strain etc. [42]. The increase in the band gap energy in sample C may be attributed to the decrease in grain size and higher lattice strain. [43] However, the sample B has shown a band gap lower than sample A and C, which may be due to the higher In content as compared to that of sample C.

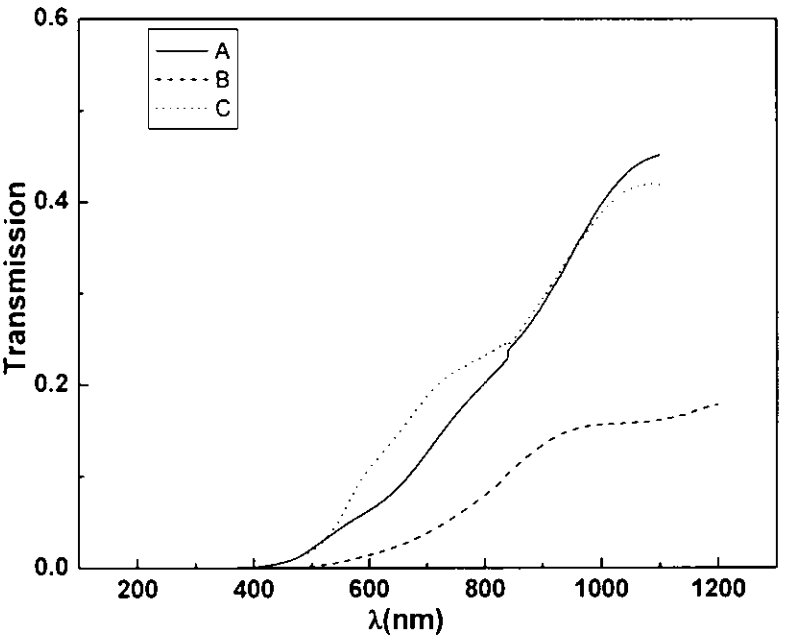

Figure: 3.4 Optical transmission spectra of samples A, B and C.

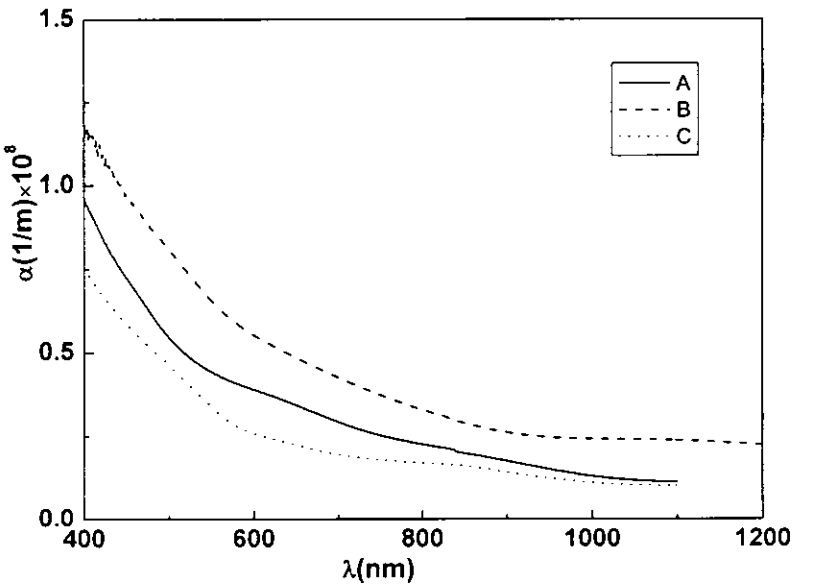

Figure: 3.5 Absorption spectra of samples A, B and C.

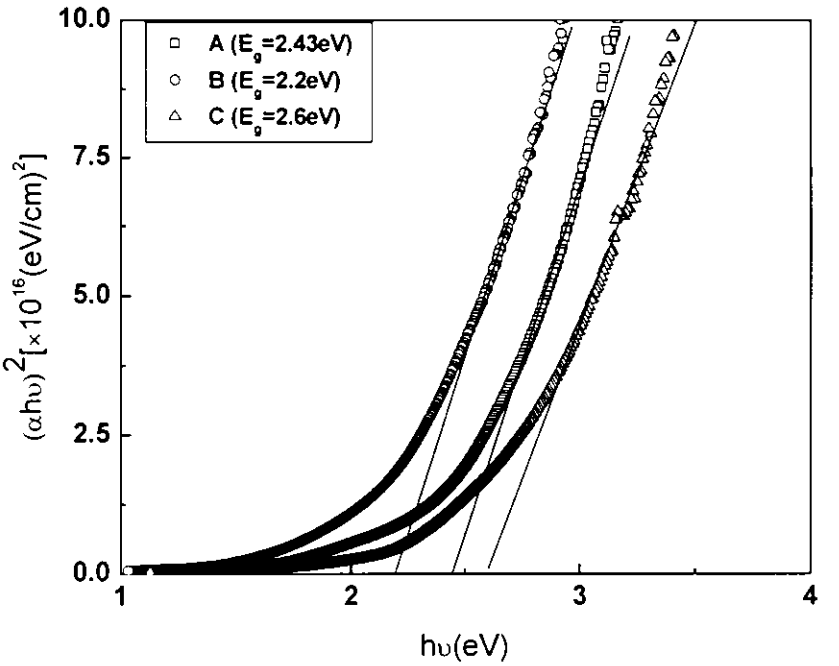

Figure: 3.6 Plot of α as function of photon energy of samples A, B and C

3.1.4. ELECTRICAL ANALYSIS

3.1.4.1. I-V CHARACTERISTICS

The I-V characteristics of ZnSe thin films of B 1 in dark as well as under illumination are shown in Fig. 3.7. (a, b). It can be seen from this figure that these films are low resistance and shown ohmic behaviour. The sample C has shown highest current values as compare to A and B thin films; where the sample B has shown least conductivity in terms of magnitude of eclectic current which flows through the sample. The conductivity of polycrystalline semiconductor thin films could be influenced by two sources; one is the grain boundaries (grain boundaries act as scattering centers for charge carriers) and the other is the charge carrier concentration (electrons/holes). The grain size in sample A and B is higher than that of sample C; higher the grain size smaller will be the grain boundaries and lower the resistance. Since sample C has smallest grain size so highest number of grain

boundaries but it has higher conductivity, therefore, the possible reason of higher conductivity of these samples is the high carrier concentration supplied by the diffused indium as compared to A and B thin films. As far as the I-V measurements in dark are concerned there was very little effect on the conductivity of the samples, which shows that the film are not very much sensitive to darkness.

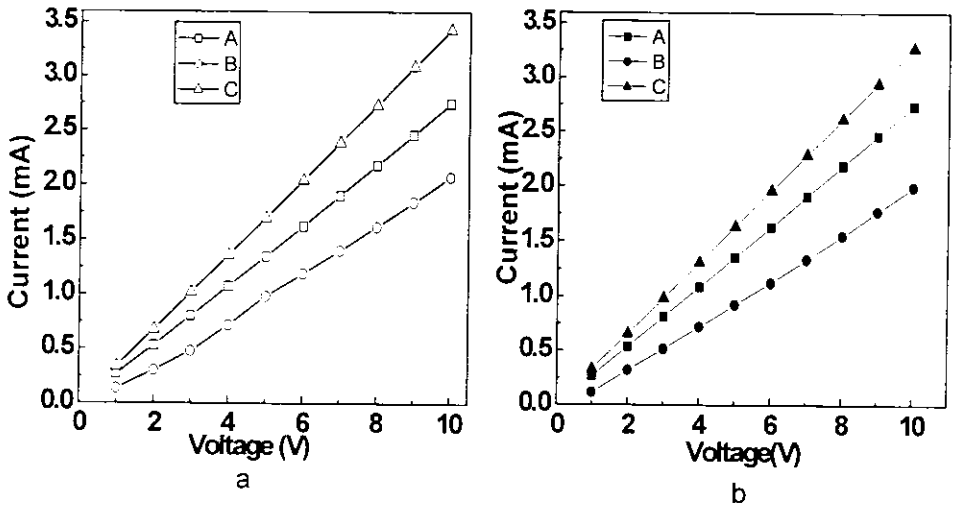

Figure: 3.7 I-V characteristics of ZnSe/ITO samples (as prepared) in (a) light (b) dark

3.1.4.2. PHOTOCURRENT AND PHOTODECAY

Figure 3.8 shows the current measurement under dark and illumination. At t=0 when the light was switched ON, there is a rise in the current through the B and C thin films. The excess carriers have been produced due to the illumination of the sample which is called the photocurrent. A gradual decay in photocurrent was observed when the light was switched OFF; it took five minutes for the current to decay to its initial values at t=0. The rise of current in the light is called photocurrent where as the decrease in photocurrent when illumination was removed is called photo decay. This behaviour which is observed in semiconductor is due to the presence of defects in the

crystals which may form electronic states (called trapping/recombination centers) in the forbidden energy gap. In presence of high density of recombination centers the rise time and fall time of photocurrent is decreased whereas the trapping centers act to prolong the decay of photocurrent. [44] In the case of ZnSe thin films B and C, there is very slow decay of the photocurrent which indicates the presence of trapping centers in the material. The A thin film has shown a slow decay which can be due to a large number of trapping centres. According to semiconductor physics the recombination rate and carrier lifetime are proportional to the density of recombination centers and carrier concentration and inversely proportional to the density of recombination centers respectively.

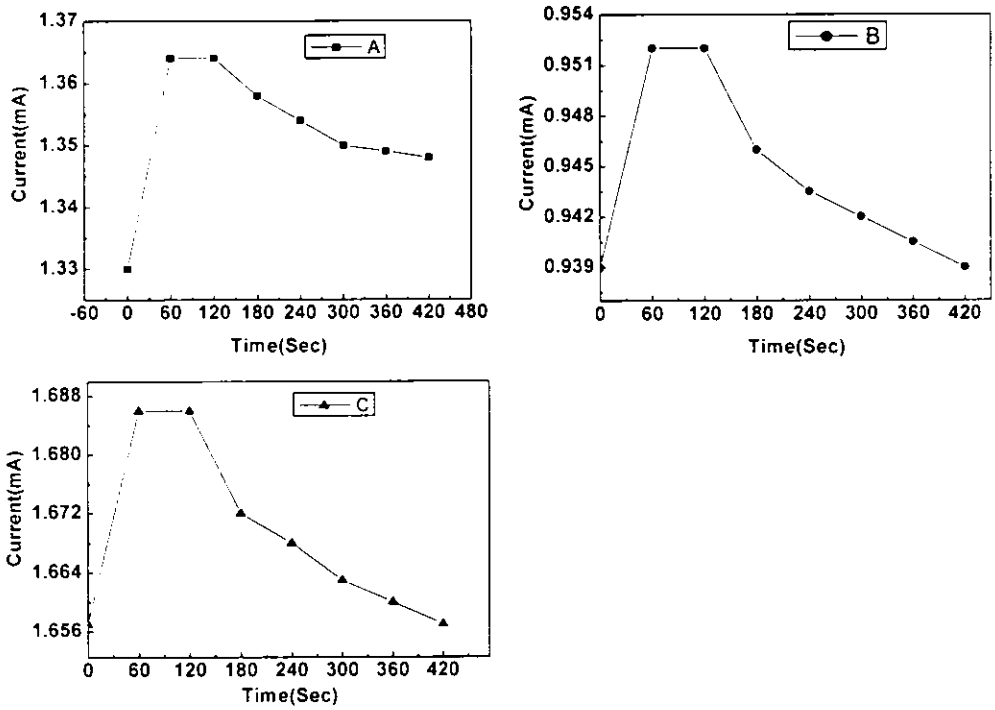

Figure: 3.8 Photocurrent rise when placed under illumination and decay in darkness after illumination in as prepared samples (a) A, (b) B, (c) C.

3.1.4.3. PHOTOSENSITIVITY

The photosensitivity of a semiconductor is the response of a semiconductor to illumination. It is defined as

$$S = \frac{I_{light} - I_{dark}}{I_{dark}}, \quad \text{..... 3.5}$$

Where I_{light}, I_{dark} are the currents through semiconductors under illumination and dark, respectively. The plot of photosensitivity versus thickness of ZnSe thin films is shown in Fig. 3.9. The figure shows that B and C thin films are more photosensitive as compared to the A thin film. In semiconductors the trapping centers which trap holes, help to increase the life time of electrons in conduction band and results in a net increase in the photocurrent. Therefore, in B and C thin films the trapping centers possibly have trapped holes, which have increased the photosensitivity of these films.

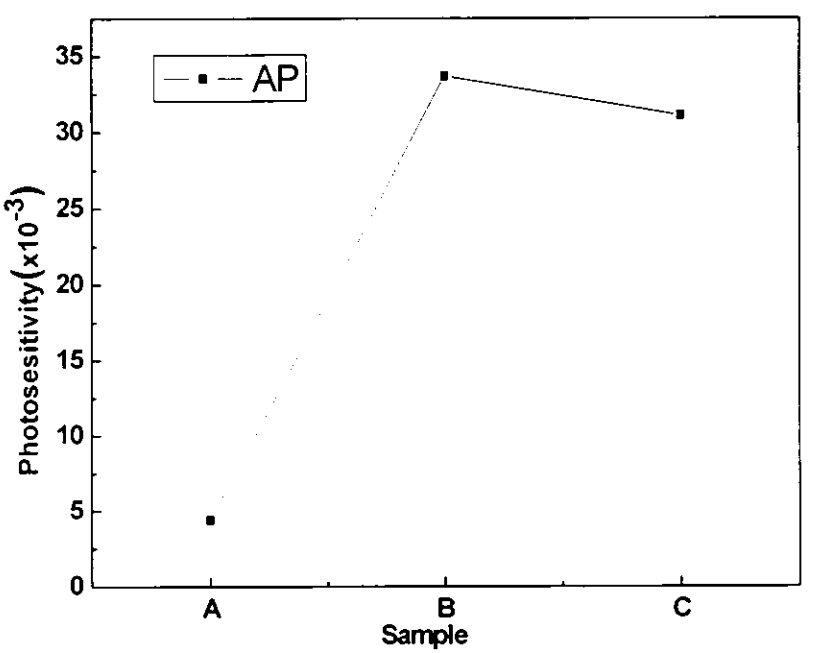

Figure: 3.9 Variation of photosensitivity samples A, B and C of ZnSe/ITO (as prepared)

3.2. SECTION-2

In B-2 the annealed samples of B1 have been discussed. The ZnSe/ITO/glass thin film samples were annealed in air at 100, 200 and 300°C for one hour. The objective of the annealing experiments was to improve the electrical properties of these samples and to study its effect on their structural properties. In the following results of the annealing experiments have been discussed.

3.2.1. STRUCTURAL CHARACTERIZATION

3.2.1.1. X-RAY DIFFRACTION

The XRD of one of the ZnSe samples annealed in air at 300°C is shown in Fig.3.10. The XRD of sample C was chosen due to its higher thickness. It can be seen from this figure that although the cell parameter has not been changed but some extra peaks have been appeared which correspond to ITO and In_2O_3. Indium possibly has reacted with the oxygen in air to form its oxide.

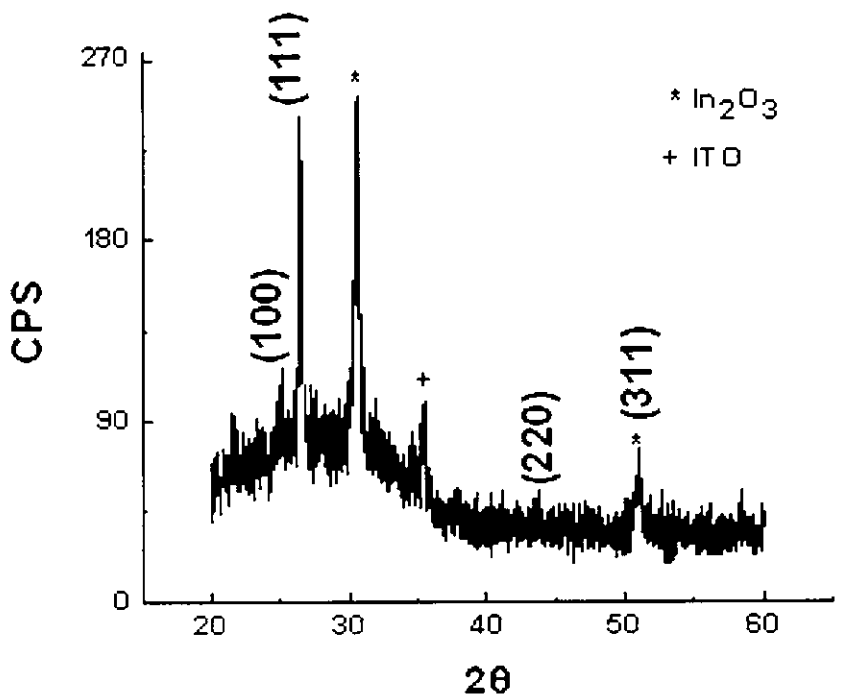

Figure: 3.10 XRD patterns of sample C annealed at 300°C

The (111) peak was used to calculate the grain size, lattice strain and dislocation density of air annealed ZnSe sample. These calculations have shown an increase in grain size which is usually observed after annealing [45]. The lattice strain and the dislocation density were decreased after air annealing. The structural parameters are given in Table 1.

3.2.1.2. RUTHERFORD BACKSCATTERING SPECTROSCOPY:

The RBS spectra of A, B, and C samples were taken after air annealing to see the effect of air annealing on the films. It was observed from this analysis that thickness of sample A and B have been decreased as shown from the decrease in the area under the peaks. Whereas, there is a diffusion of the ZnSe thin film into the ITO/glass substrate in the case of sample C, which is in agreement with the XRD analysis which has shown the presence of ITO peak.

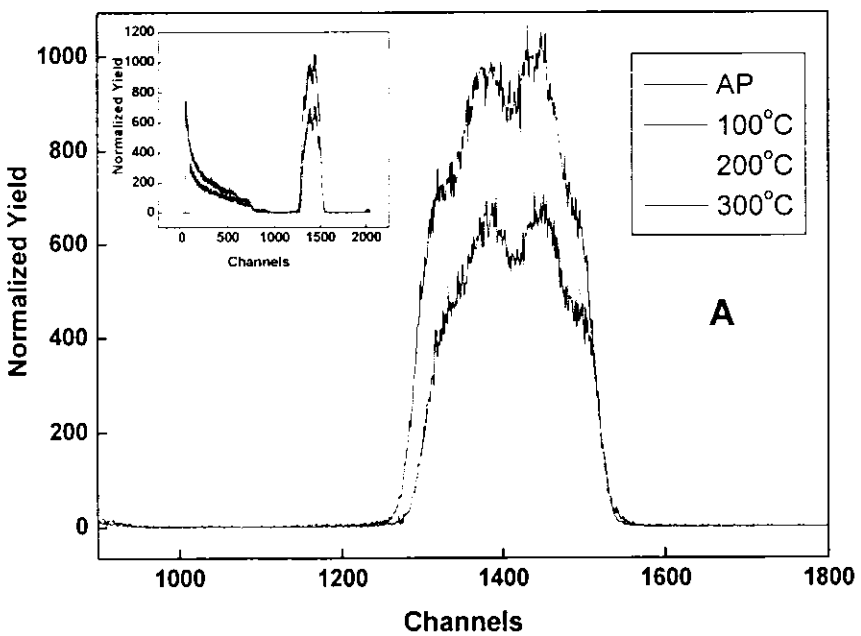

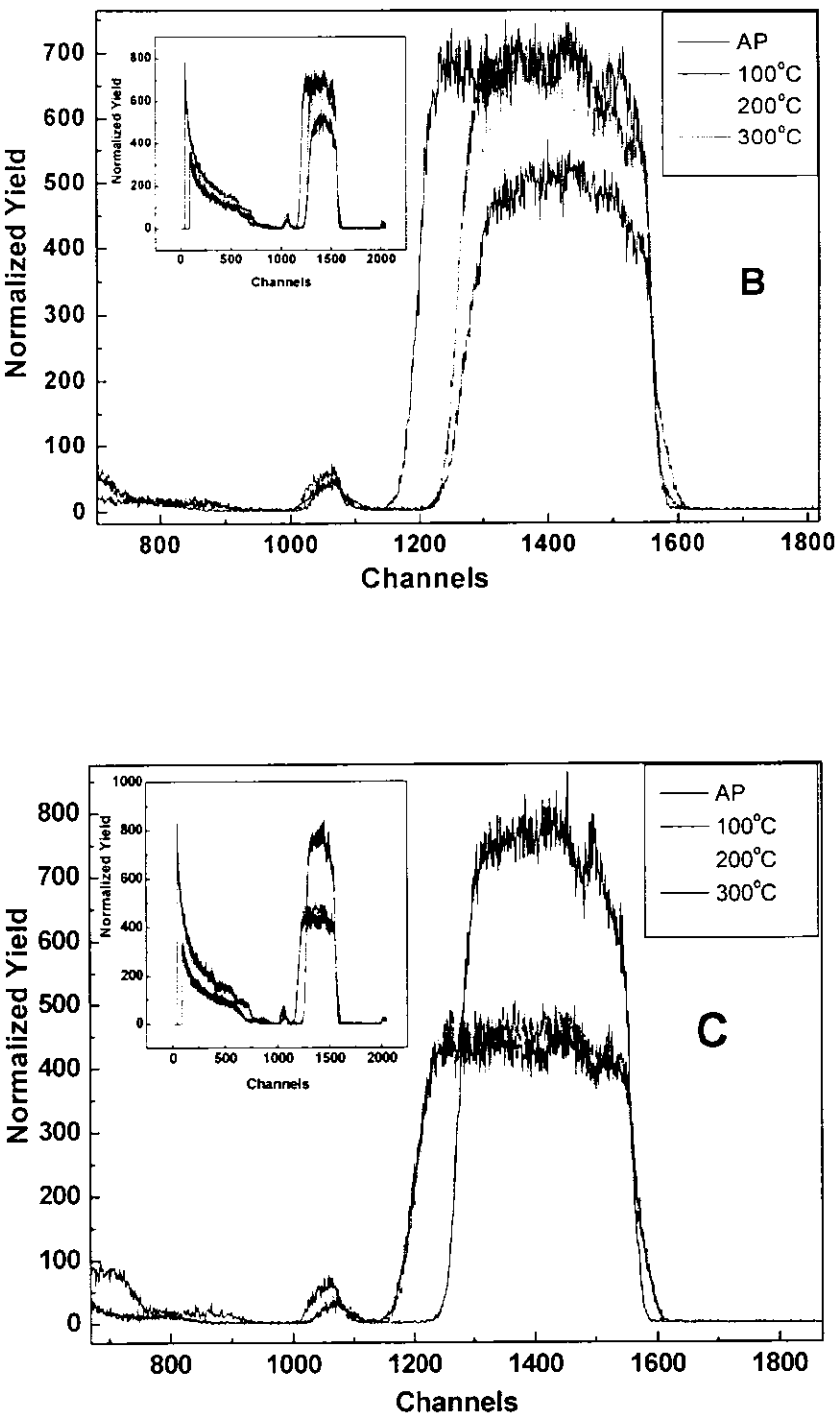

Figure: 3.11 RBS spectra of annealed ZnSe/ITO Samples (a) A,(b) B and (c) C

3.2.2. ELECTRICAL ANALYSIS

3.2.2.1. I-V CHARACTERISTICS

Sample A

I-V characteristics of ZnSe thin films, sample A annealed at 100°C, 200°C and 300°C, under illumination as well as in dark are shown in Fig. 3.12. (a, b). It can be seen from this figure that there is an increase in the film conductivity with the increase in the annealing temperature. Since it is known that the conductivity is influenced by grain size as well as the carrier concentration, hence the possible reason for this behaviour can be due to the increasing grain size with annealing temperature. The increase of grain size with annealing has been verified by XRD data analysis. The second possible reason could be the diffusion of indium in ZnSe thin film which can increase the charge carrier concentrations but we did not observe further diffusion of indium or Sn in to the film from the RBS spectra, therefore, the most possible reason of increase in conductivity might be the increase in grain size. The increased grain size reduces the number of grain boundaries and hence the resistance of the material. The samples have shown same behaviour in the dark and did not observe any improvement in the photosensitivity of the films after annealing.

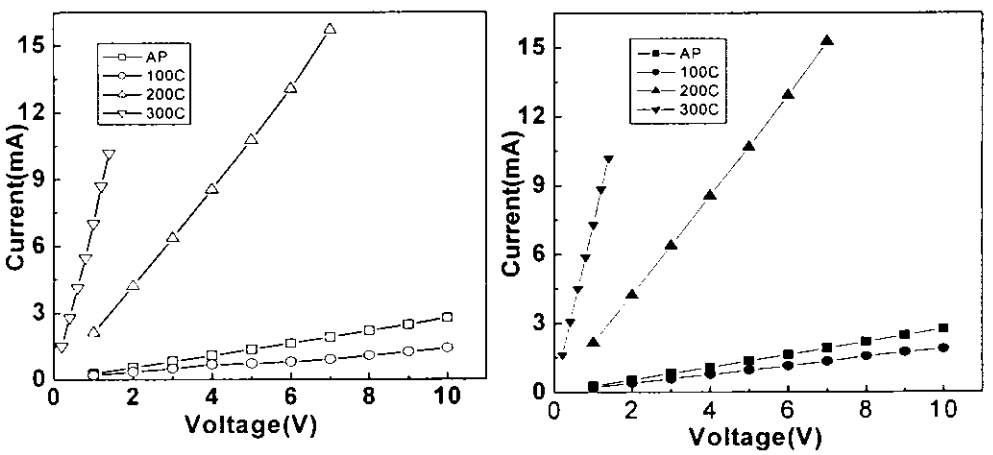

Figure: 3.12 I-V characteristics of ZnSe/ITO of sample A after annealing in (a) light (b) dark

Sample B

I-V characteristics of ZnSe thin films, sample B annealed at 100, 200 and 300°C, under illumination as well as in dark are shown in Fig. 3.13 (a, b). It can be seen from this figure that these films are low resistance and ohmic in nature. The conductivity of the samples has been increased with the increase of annealing temperature above 100°C. There is very little change in the conductivity after annealing at 100°C. The increase in conductivity after 300°C annealing is very high and at very low applied voltage (5V) current through the sample exceeded than that of lower temperature anneals, which shows that 300°C is the appropriate temperature to increase the conductivity of the samples without changing the structure of the material. The measurements in dark have shown the similar response as observed for the case of sample A.

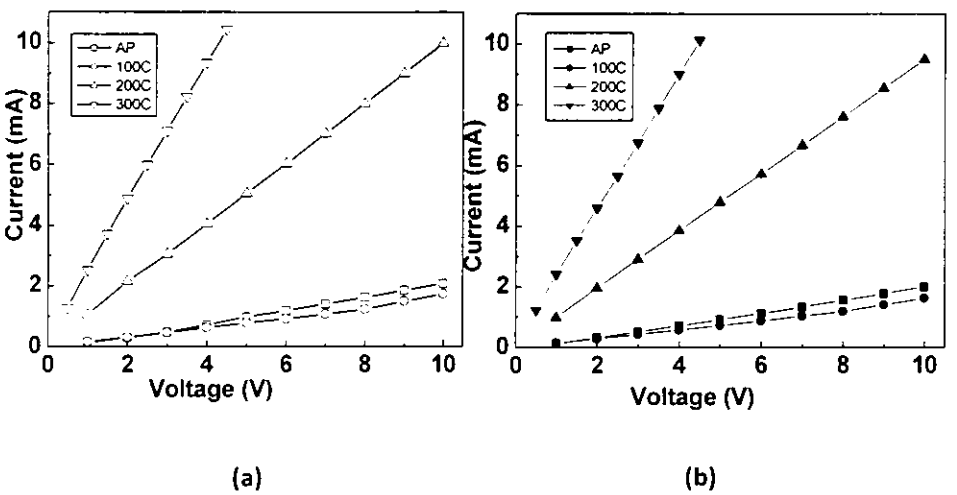

Figure: 3.13 I-V characteristics of ZnSe/ITO of sample B after annealing in (a) light (b) dark

Sample C

I-V characteristics of ZnSe thin films, sample C annealed at 100, 200 and 300°C, under illumination as well as in dark are shown in Fig. 3.14. (a, b). There is an increase in conductivity after annealing above 100°C. It can also be seen from this figure that the increase in current with the applied voltage is very high even at small

applied voltages as compared to the as-prepared and 100°C annealed sample. It was observed from the XRD analysis that the grain size of the as-prepared sample C is small as compared to that of sample A and B, therefore, such a huge increase in conductivity could possibly be due to two reasons; one is the increase in grain size after annealing (Which is also observed from XRD data analysis) and the second is the increased intermixing of ZnSe/ITO layers as observed from the RBS analysis. The intermixing of the two layers might have increased the charge carriers. Thin film n-type As far as the I-V measurements in dark are concerned there was very little effect on the conductivity of the samples, which shows that the film are not very much sensitive to darkness.

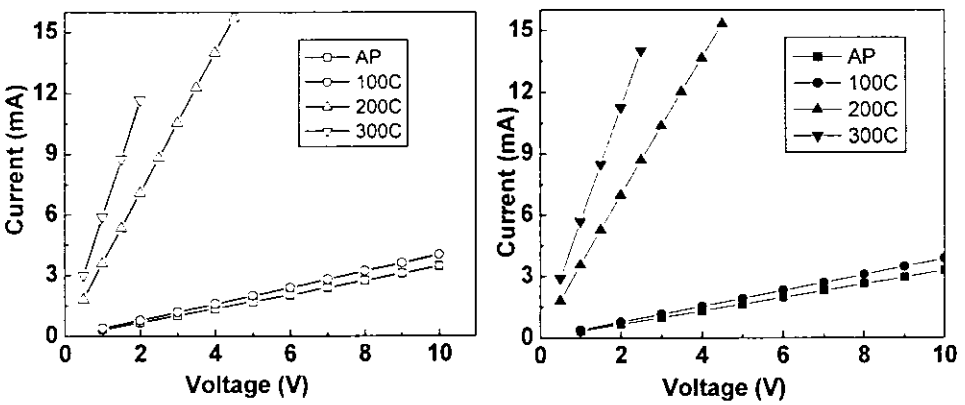

Figure: 3.14 I-V characteristics of ZnSe/ITO of sample C after annealing in (a) light (b) dark

The I-V characteristics of ZnSe thin films samples A, B and C annealed at 100, 200 and 300°C are compared in Figs. 3.15-3.17 (a and b). It can be seen from this figure that at each annealing temperature the conductivity of the ZnSe film with highest thickness (sample C) has higher conductivity, whereas that of sample B is least. However, at 300°C annealing conductivity of sample A and C is equal but still larger than that of sample B. The comparison of I-V curves of ZnSe thin films also shows that the annealing of samples at 200°C has resulted in maximum increase in the conductivity of the films. We have seen from the XRD of 300°C sample that in

addition to ZnSe crystalline phase there also exist ITO and In_2O_3 phases, with an increase in grain size. The inclusion of the impurity phases might have created donor/acceptor states which can produce majority carriers in the material and hence the higher conductivity at room temperature. However, from the RBS analysis we can see that there is a decrease in the peak counts after annealing, which would have changed the Zn to Se ratio and hence the charge carrier concentration in the sample.

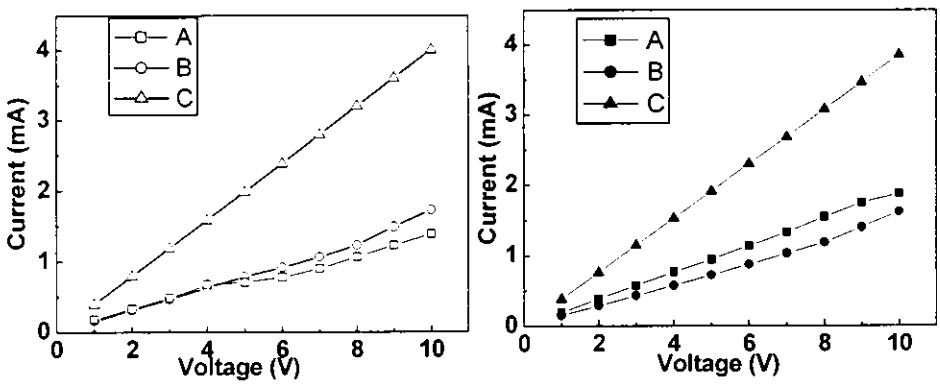

(a) (b)

Figure: 3.15 I-V characteristics of ZnSe/ITO samples annealed at 100°C in (a) light (b) dark

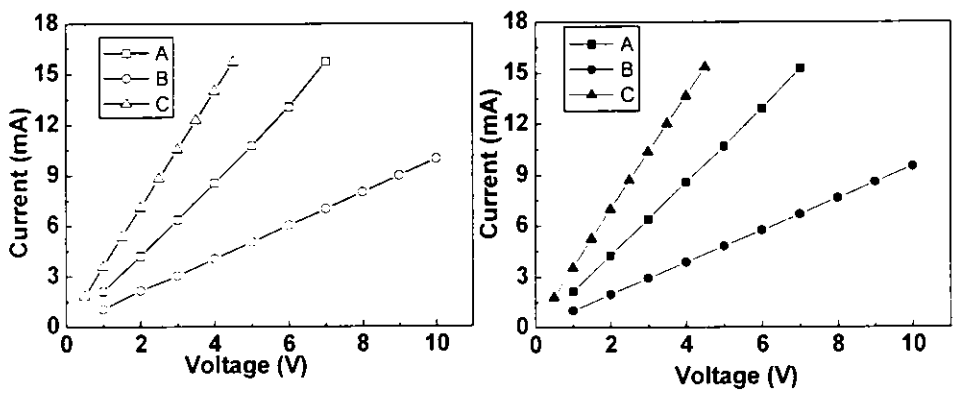

(a) (b)

Figure: 3.16 I-V characteristics of ZnSe/ITO samples annealed at 200°C in (a) light (b) dark

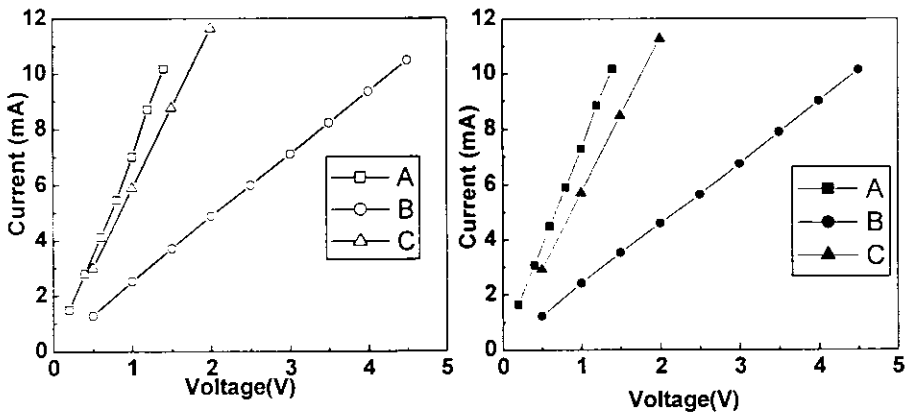

(a) (b)

Figure: 3.17. I-V characteristics of ZnSe/ITO samples annealed at 300°C in (a) light (b) dark

3.2.2.2. PHOTOCURENT AND PHOTODECAY

Fig. 3.18 shows the response of ZnSe thin films under light and then in dark after annealing at 100°C. At t=0 when the light was switched ON, there is a rise in the photo current through the sample B and C. It can be seen from this figure that a sharp decay in photo current was observed during the first minutes after the light was switched OFF and then a gradual slow decay in photocurrent in successive minutes was observed; it took five minutes for the current to decay to its initial values at t=0. In the as-prepared sample such sharp decay of current was not observed, which shows that after air annealing some trapping centers have been produced, which quickly trapped the excess carriers when the photo excitation was removed and later on those trapped carriers have been released gradually producing a slow decrease of the photocurrent. It can be seen from this figure that sample A shows an anomalous behaviour, instead of current rise after the application of photo excitation there is a sharp current fall and after the illumination was switched OFF there is a current rise in the dark during the measurement time. The possible reason is that some defects have been generated after annealing which act as trapping centres which trapped excess carriers and after the illumination is switched OFF the trapped carriers have been

released. This result has also shown that the external excitation source (i.e.light) played a negative role.

In Fig. 3.19 the photo decay in sample A, B, and C after 200°C annealing has been compared. These results show that annealing at 200°C did not affect the behaviour of photo decay in sample A and B. The possible reason of such behaviour is that the trapping centers produced are of the same type as in the as-prepared samples. However, in the case of sample C two steps have been observed in the photo decay region showing the presence of two different types of trapping centers.

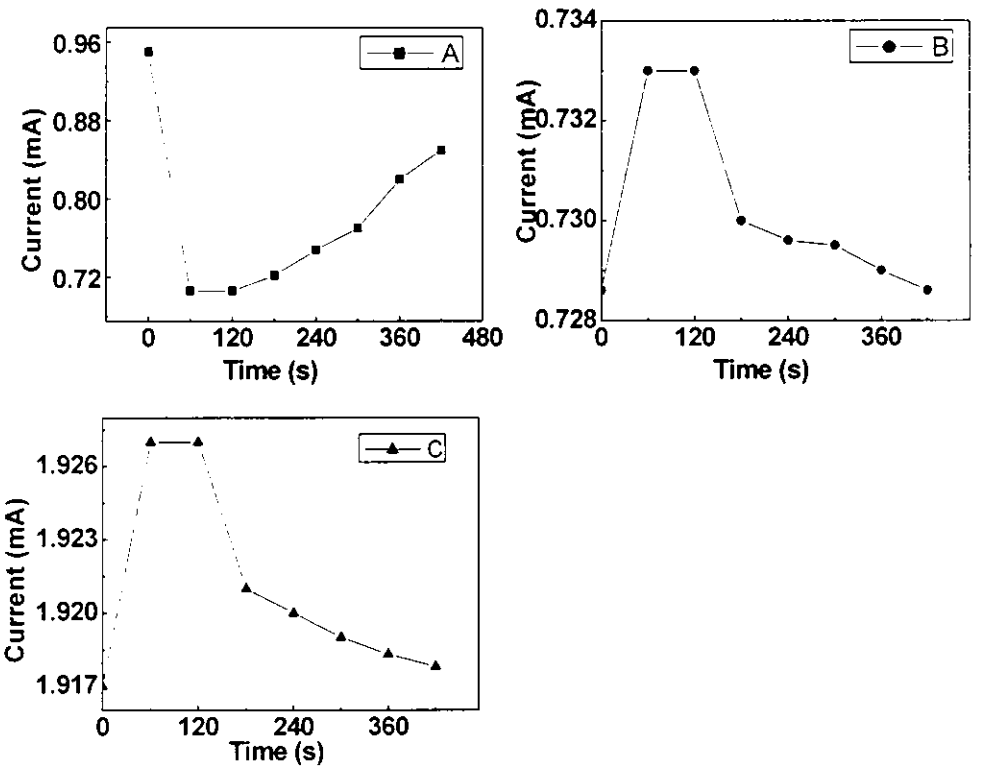

Figure: 3.18. Photocurrent rise when placed under illumination and decay in darkness after illumination of samples (a) A, (b) B, (c) C annealed at 100°C

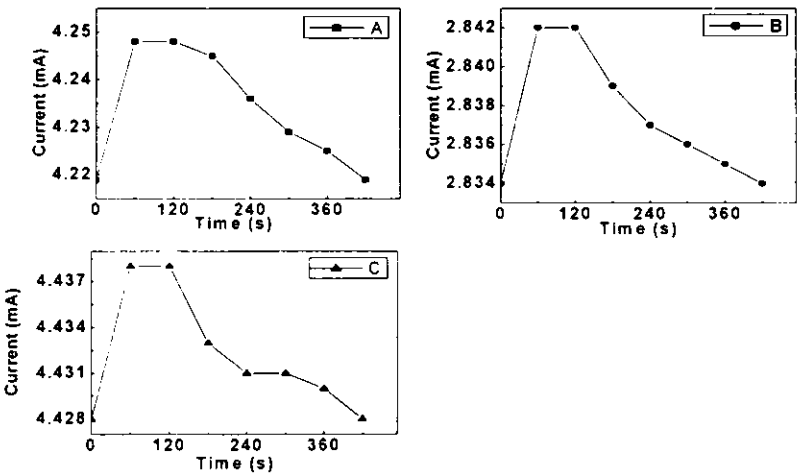

Figure: 3.19. Photocurrent rise when placed under illumination and decay in darkness after illumination of samples (a) A, (b) B, (c) C annealed at 200°C.

The photo decay measurements of ZnSe thin film samples A, B and C after 300°C annealing are shown in Fig. 3.20. In sample B the photo decay is linear with time from the start of the dark region. The sample A have shown a decrease in current after illumination and gradual increase in dark and C have shown a sudden fall in current in first min and then a slow decay. In sample A and C similar behaviour was observed after 100°C anneal respectively.

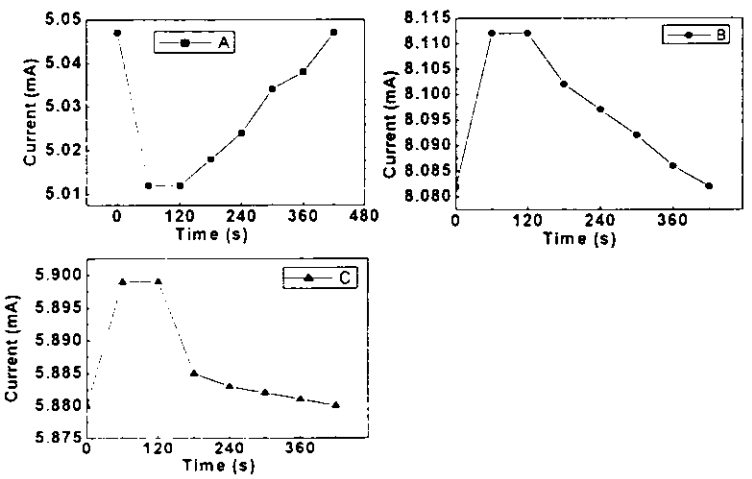

Figure: 3.20. Photocurrent rise when placed under illumination and decay in darkness after illumination of samples (a) A, (b) B, (c) C annealed at 300°C.

3.2.2.3. PHOTOSENSITIVITY

The plot of photosensitivity versus thickness of ZnSe thin films is shown in Fig.3.21. for the samples annealed at 100, 200 and 300°C. It can be seen from this figure that the films with intermediate thickness i.e. 76nm has shown higher photosensitivity as compared to sample A and C. However, the photosensitivity has been decreased in all the samples after annealing as compared to as-prepared samples. In semiconductors the trapping centers which trap holes, help to increase the life time of electrons in conduction band and results in a net increase in the photocurrent. Therefore, in B and C thin films the trapping centers possibly have trapped holes, which have increased the photosensitivity of these films.

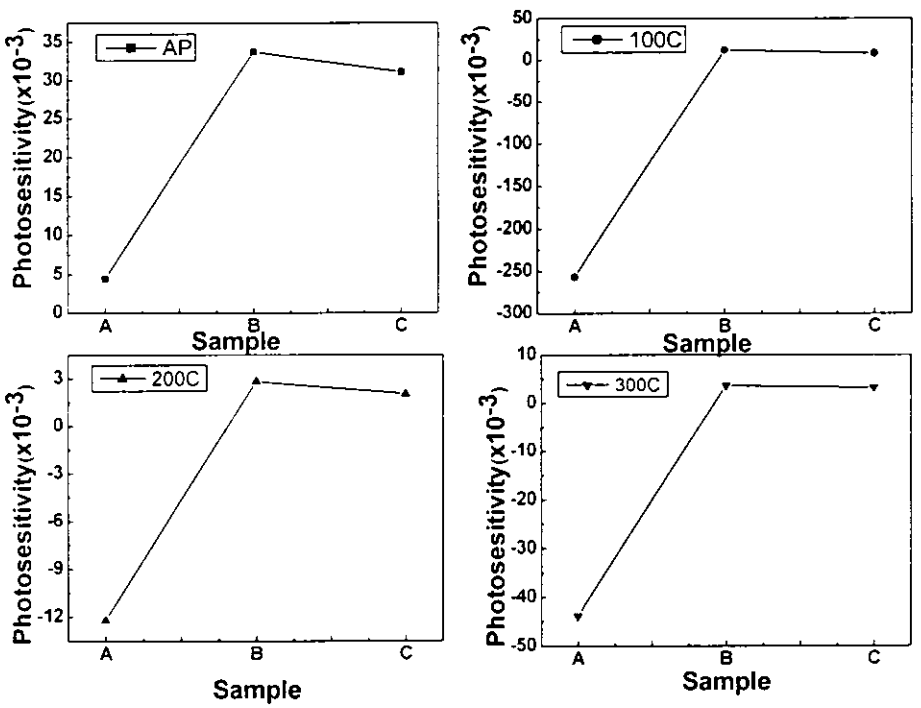

Figure: 3.21. Variation of photosensitivity samples A, B and C as prepared and annealed at 100°C, 200°C and 300°C.

3.3. SECTION-3 Ag-DOPED

In this section structural, optical and electrical analysis of ZnSe thin films deposited in B2 have been discussed. First of all the results of XRD, RBS and SEM have been discussed then the results of transmission spectroscopy are described in last results of electrical properties i.e. I-V characteristics, Photocurrent and Photo decay and photosensitivity have been discussed. In this section the samples with thickness 64, 72 and 73nm are designated with alphabets a, b and c.

3.3.1. STRUCTURAL CHARACTERIZATION

3.3.1.1. X-RAY DIFFRACTION

The XRD of one of the ZnSe samples of B2 is shown in Fig.3.22. The XRD of sample c has the highest thickness among those deposited in B2. XRD pattern of this sample shows a single fine peak at 2θ=27.14 which shows its cubic structure over amorphous glass. Structural parameters have been calculated which are shown in Table 1. It can be seen that the grain size is about 33nm. This shows its good quality of deposition. The lattice parameters were found to be 5.676 which is very close to the already reported value [37].

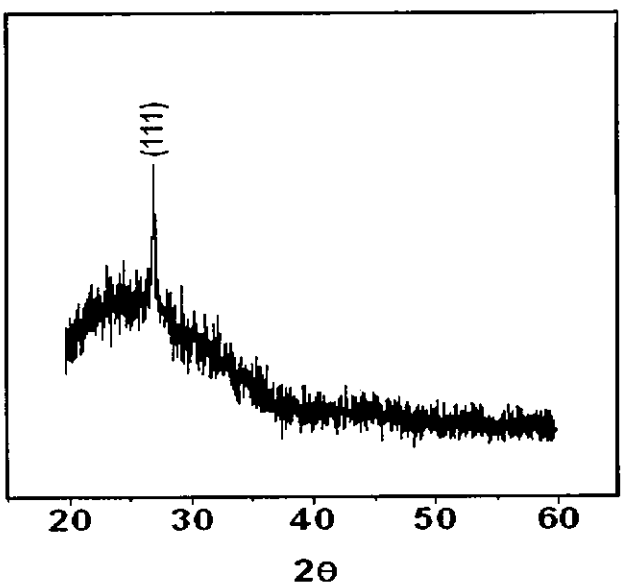

Figure: 3.22. XRD Pattern of sample "c"

3.3.1.2. COMPOSITION, THICKNESS AND MICROSTRUCTURE:

Rutherford Backscattering Spectroscopy (RBS) was used to measure the composition and thickness of as deposited thin films. The RBS spectra of as prepared sample a, b and c along with their simulation spectra are shown in Fig. 3.23. Thickness and composition of these samples were calculated by using the simulation codes RUMP and SIMNRA. Results are shown in table. 3 (a). The thickness of sample a, b and c (as deposited) are calculated to be 64nm, 72nm and 73nm. Compositional analysis shows that Zn to Se have almost same ratio in all the samples.

RBS spectra of these samples after doping are shown in Fig. 3.24. The thicknesses of these samples are 79nm, 48nm (in two layers) and 43nm. The results are shown in table. 3. (b). The RBS analysis shows that there is uniform diffusion of Ag in thin film of sample a and c while in sample b Ag components are at surface and have not completely diffused in the film. The Ag component in sample is about 32% while in b and c it is about 22% which is much less than that of sample a.

The microstructure of the ZnSe thin films deposited on glass substrate was studied through scanning electron microscopy (SEM). Two samples were selected for this purpose. One sample having least thickness "a" and second having largest thickness "c". The SEM micrographs are shown in Fig.25. (a, b). It can be seen from these images that there is full coverage of the glass substrate by the film with SEM selected resolution with small amount of clusters on the film surface of sample c.

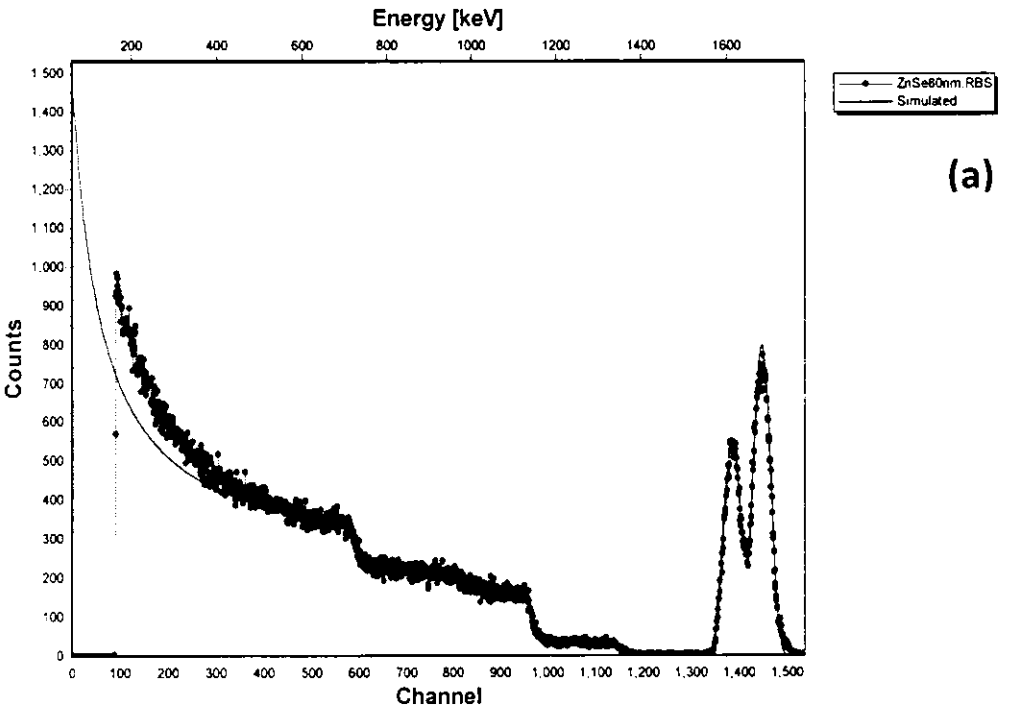
Energy [keV]
200 400 600 800 1000 1200 1400 1600
Counts
0 100 200 300 400 500 600 700 800 900 1,000 1,100 1,200 1,300 1,400 1,500
Channel
ZnSe60nm.RBS
Simulated
(a)

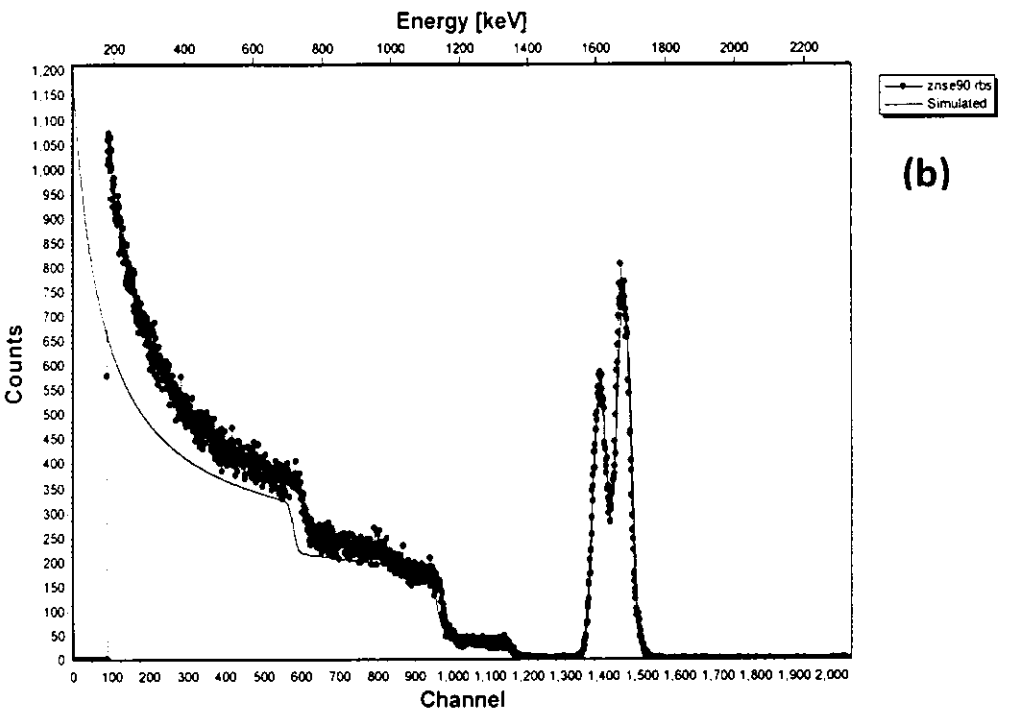
Energy [keV]
200 400 600 800 1000 1200 1400 1600 1800 2000 2200
Counts
0 100 200 300 400 500 600 700 800 900 1,000 1,100 1,200 1,300 1,400 1,500 1,600 1,700 1,800 1,900 2,000
Channel
znse90 rbs
Simulated
(b)

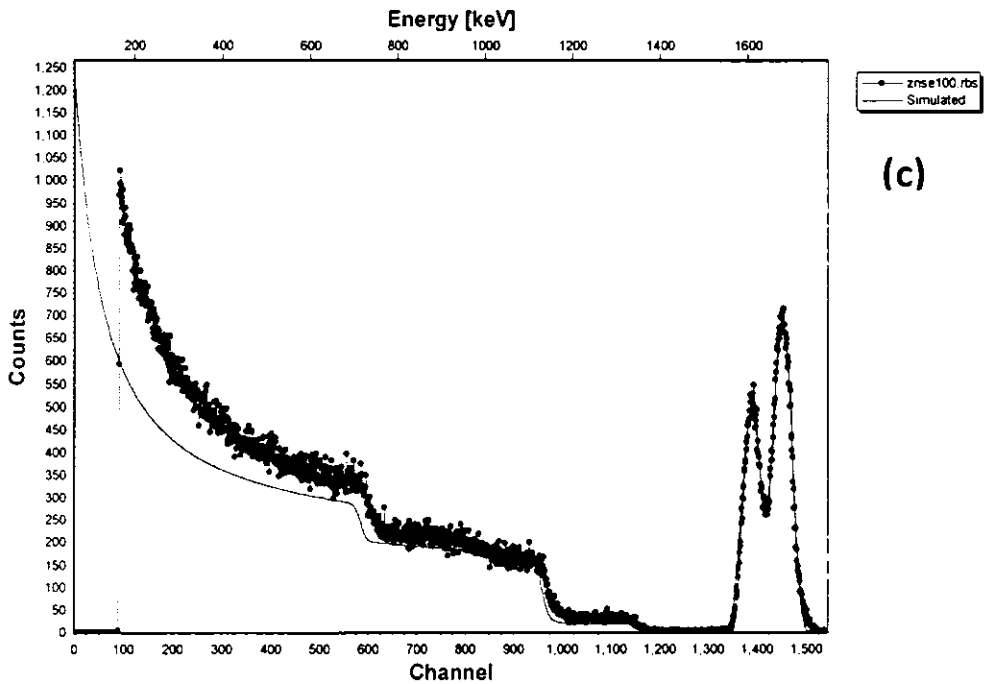

Figure: 3.23. RBS spectra with simulated spectra of undoped samples (a) a,(b) b and (c) c

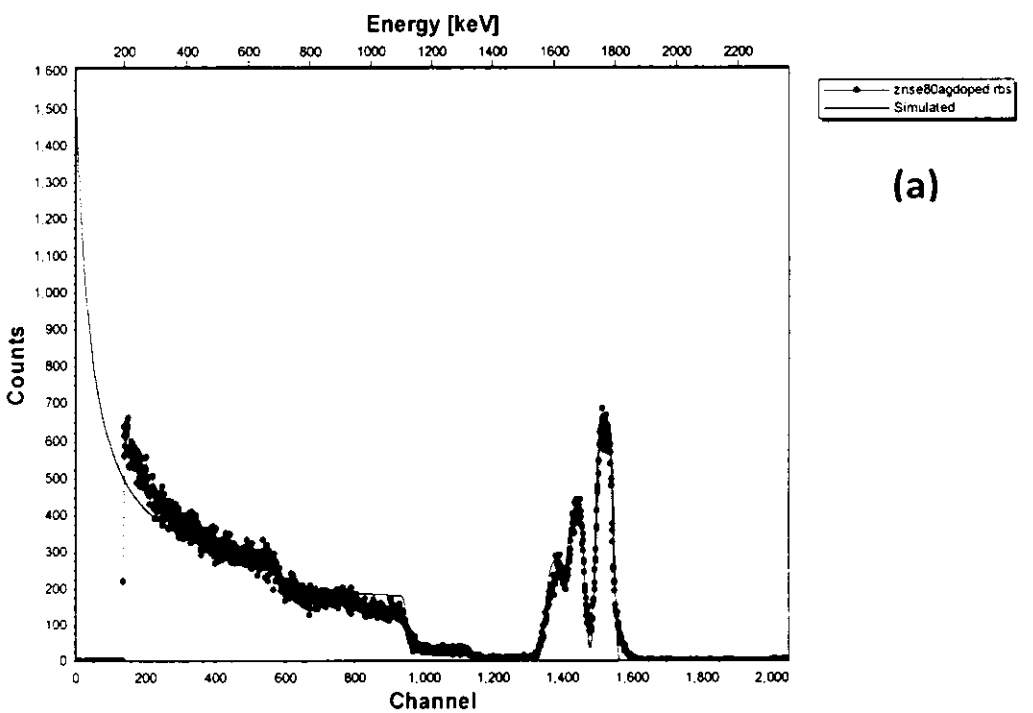

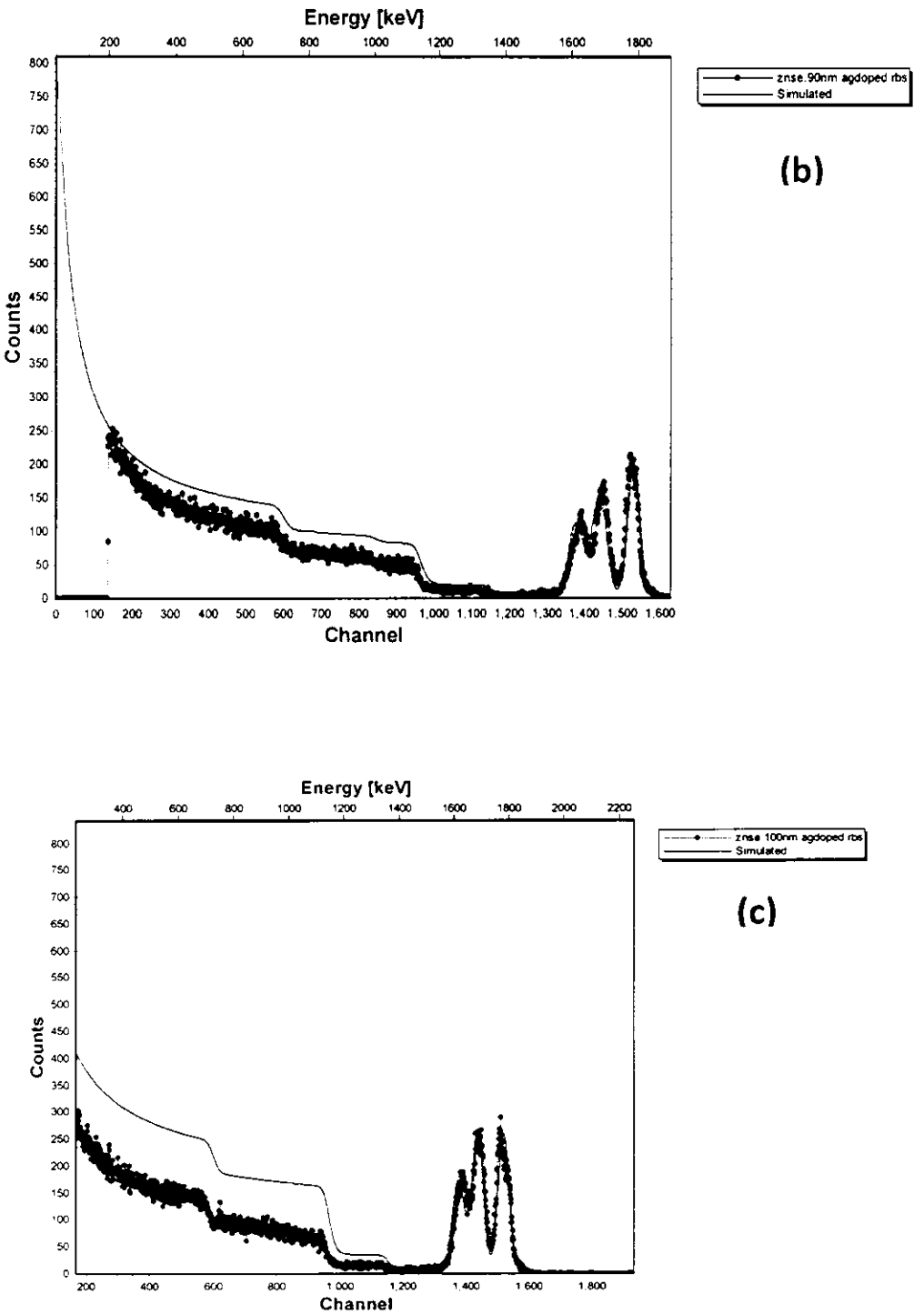

Figure: 3.24. RBS spectra with simulated spectra of samples (a) a,(b) b and (c) c after Ag doping

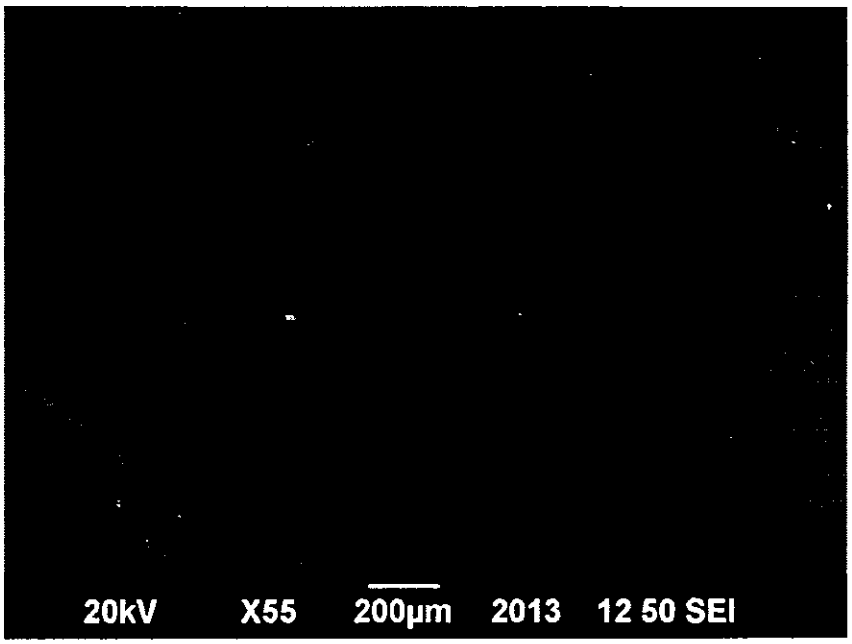

(a)

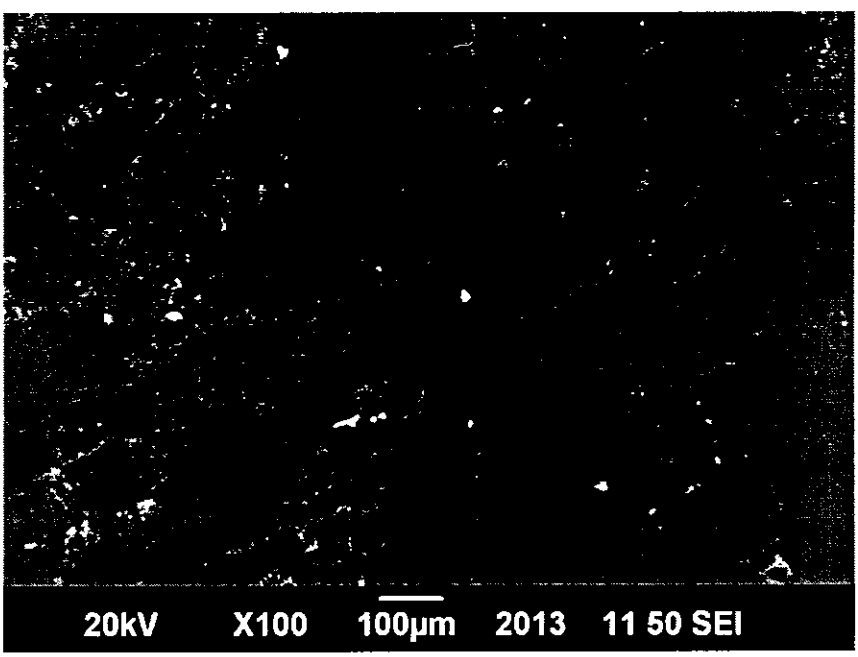

(b)

Figure: 3.25. SEM micrograph of samples (a) a and (b) c

Sample	a (As-deposited)			b (As-deposited)			c (As-deposited)		
Layer 1	th	Zn%	Se%	th	Zn%	Se%	th	Zn%	Se%
	64nm	48	52	72nm	49.5	50.5	73nm	49.1	50.9
Sample	a (Ag-doped)				b (Ag-doped)			c (Ag-doped)			
Layer 1	th	Zn %	Se %	Ag %	th	Zn %	Se %	Ag %	th	Zn %	Se %	Ag %
	79nm	32	36	32	30nm	31	33	36	43nm	37	42	21
Layer 2					Th	Zn %	Se %					
					18nm	50	50					

Table: 3.3. Table of the thickness and percent composition of different elements present in each layer in ZnSe as prepared and Ag doped samples data obtained from Rutherford backscattering spectroscopy (RBS)

3.3.2. OPTICAL ANALYSIS

The optical spectra of a, b and c samples in the wavelength range 200-1200nm are shown in Fig. 3.26. We can see that the optical transmission decreases with the increase of film thickness.

The effects of reflection and transmission losses can be due to glass substrate and film thickness. The absorption coefficients as a function of incident photon energy are shown in Fig. 3.27. It can be seen from this figure that the absorption coefficient increases with the increase of film thickness.

The energy gap E_g of the films was calculated from $(\alpha h\nu)^2$ vs hν plots as shown in Fig. 3.28. by assuming direct band gap material. By drawing the intercepts from the linear portion of the $(\alpha h\nu)^2$ vs hν curves. The x-intercepts values are selected as the energy gap of each sample. The calculated band gap values are 4.30, 4.40 and 4.41eV for samples a, b and c respectively. It can be seen that with the increase of film thickness there is an increase in band gap energy which may be due to the decrease of grain size with increase of film thickness.

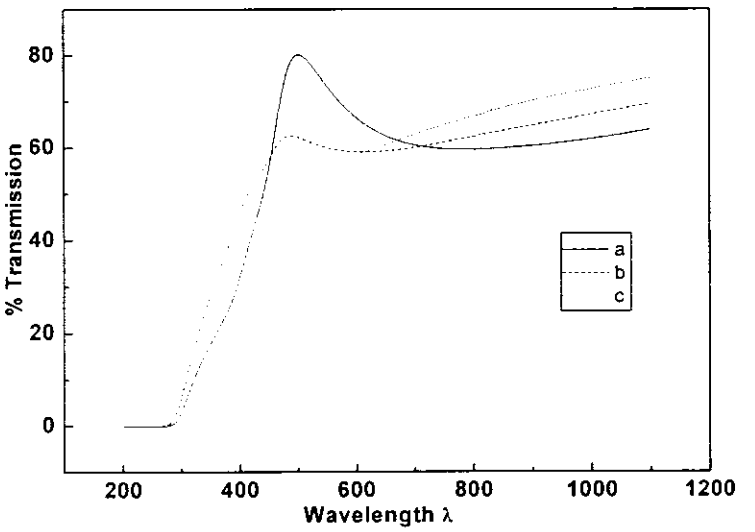

Figure: 3.26. Optical transmission spectra of samples a, b and c.

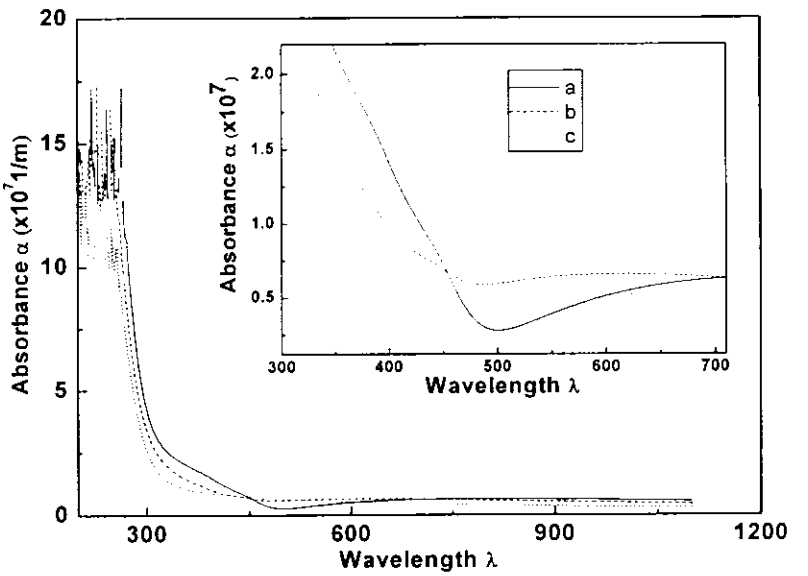

Figure: 3.27. Optical transmission spectra of samples a, b and c.

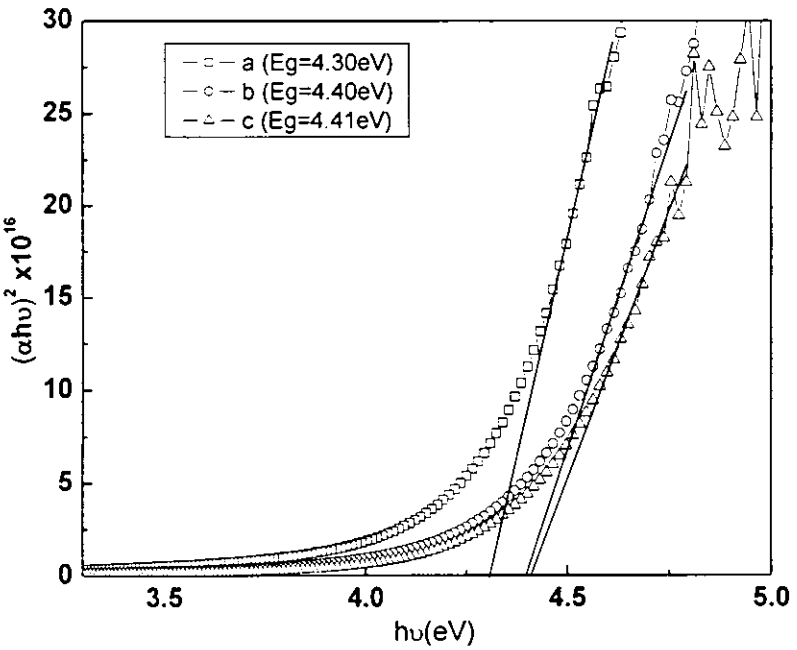

Figure: 3.28. Plot of α as function of photon energy of samples a, b and c

3.3.3. ELECTRICAL ANALYSIS

3.3.3.1. I-V CHARACTERISTICS

The I-V characteristics of samples a, b and c doped with Ag in light and dark are shown in Fig. 3.29. (a, b). Figure 3.29 shows that the films are low resistance and ohmic in nature. The sample a has shown highest current values than b and c. It can be seen from the graph that the value of current is approximately equal in b and c. The possible reason of highest current values in a can be due to the presence of higher amount of Ag contents which is verified by RBS data. After doping of Ag the thickness have been reduced also fewer amount of Ag can be the reason for lower conductivity in sample b and c. I-V measurements in dark and light shows that the films are not are much sensitive to dark.

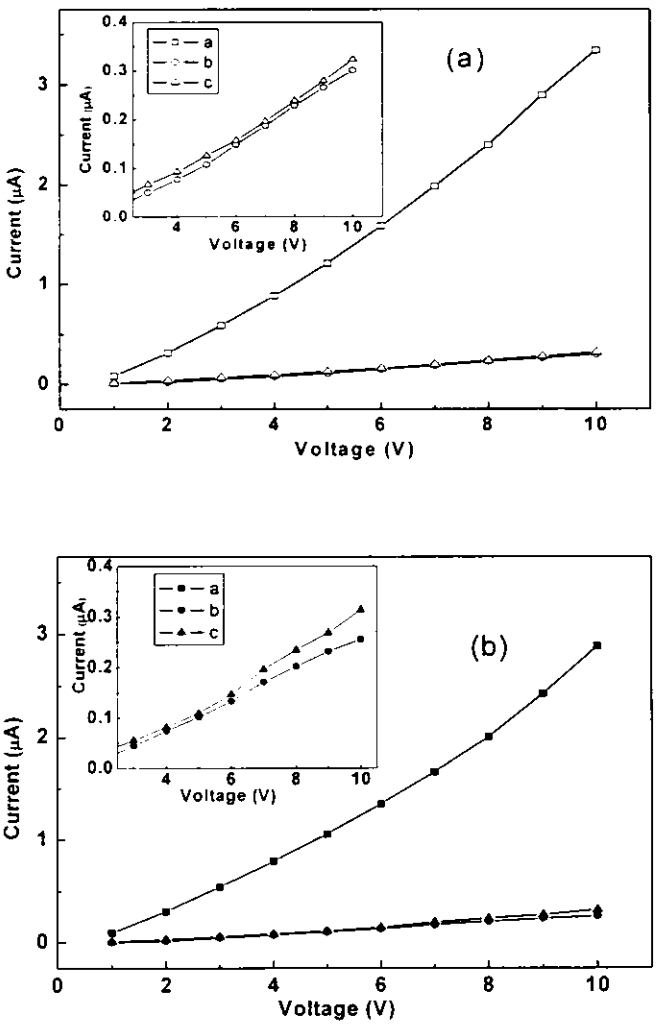

Figure: 3.29. I-V Characteristics of ZnSe samples doped with Ag in (a) light (b) dark

3.3.3.2. PHOTOCURRENT AND PHOTODECAY

Fig.3.30. shows the current measurement under dark and illumination. At t=0 when the light was switched ON, there is a rise in the current through the Ag doped samples a, b and. A gradual decay in photocurrent was observed when the light was switched OFF; it took five minuets for the current to decay to its initial values at t=0. In the case of sample c, in first minute a slow decay and then a relatively higher decay have been observed. In sample b a linear decay has been observed while in sample a there is very slow decay of the photocurrent which indicates the presence of trapping centers in the material

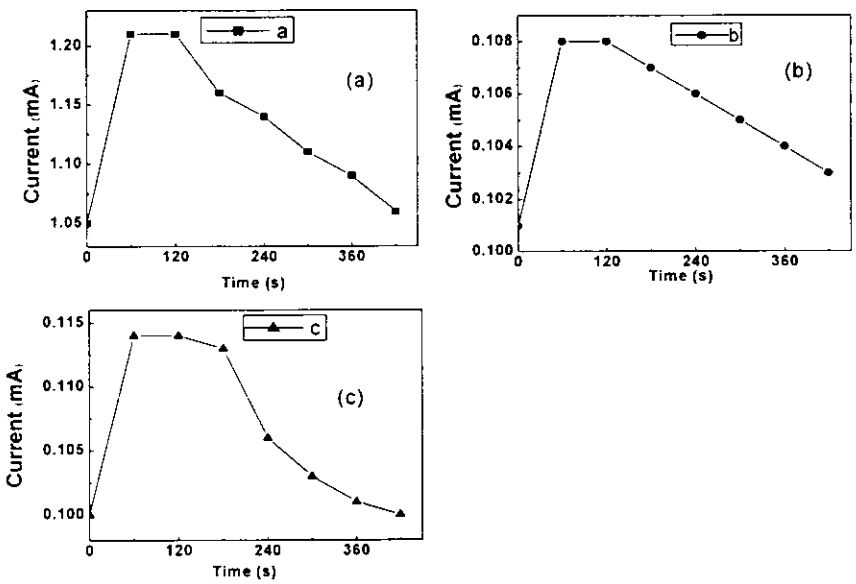

Figure: 3.30. Graph showing the thickness wise decay of current when the ZnSe doped with Ag sample is placed in darkness (a) a, (b) b, (c) c.

3.3.3.3. PHOTOSENSITIVITY

The plot of photosensitivity versus thickness of ZnSe thin films is shown in Fig.3.31. The figure shows that sample a and c are more photosensitive as compared to sample b. In samples a and c the trapping centers possibly have trapped holes, which have increased the photosensitivity of these films. While in case of sample b the lowest photosensitivity may be due the presence of Ag contents on the surface.

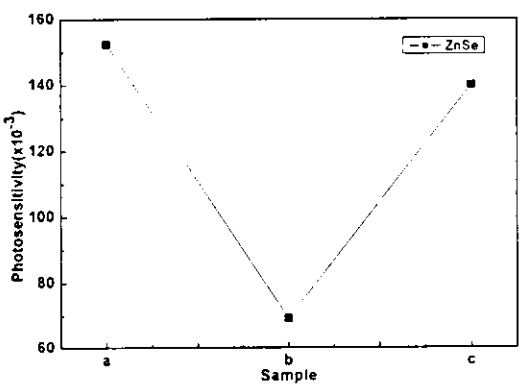

Figure: 3.31 Photosensitivity of Ag doped ZnSe samples a, b and c

CHAPTER 4

SUMMARY AND CONCLUSION

4.1. SUMMARY

1. It was observed from the structure analysis of ZnSe/ITO/glass and ZnSe/glass films that thin films with lowest thickness has the axis length is that of pure ZnSe. However, as the thickness of ZnSe/ITO/glass film is increased there is an increase in the axis length of the films, which shows that the structural properties are changed when ZnSe films are deposited on ITO coated glass substrate as compared to that of ZnSe on glass substrate.

2. The Rutherford Backscattering analysis of ZnSe/ITO/glass thin films shows that there is diffusion of In from substrate into the film. The inclusion In in the film might be the reason of high conductivity of as-prepared ZnSe/glass film. The SEM images shows good quality ZnSe/ITO/glass and ZnSe/glass films of all thickness.

3. The optical transmission spectra of ZnSe/ITO/glass show that the energy band gap of intermediate thickness is least whereas that of sample with maximum thickness is close to that of already observed Eg values. The large Eg in ZnSe may be due to decrease in grain size and higher lattice strain as compared to other samples.

4. The electrical conductivity measurement shows that ZnSe/ITO/glass films with highest thickness are more conductive that other two samples. The possible reason is higher charge carrier concentration in these samples. The photo response of ZnSe/ITO/glass shows that thin films with higher thickness i.e. B and C are more photosensitive than that of sample A. Whereas in the case of ZnSe/glass, the thin film with intermediate thickness are least photosensitive. The

annealing of samples shows that there is an increase in the electrical conductivity of all samples.

5. The electrical conductivity measurements of ZnSe/glass thin films shows that as-prepared samples are highly resistive but after silver doping the electrical conductivity of all the samples have been increased.

4.2 CONCLUSION

We can conclude from the summary of the results that ZnSe thin films become conductive when deposited on ITO coated glass substrate eliminating the need of further doping of the material. Moreover, the lattice parameters become close to that of CdTe making ZnSe a suitable window material for CdTe/ZnSe hetero-junction solar cell. It has also been concluded that thickness is not only parameter which affects the properties of ZnSe thin films, other parameter i.e. film quality , grain size, optical band gap all contribute to the over all performance of ZnSe thin films.

REFERENCES

[1] en.wikipedia.org/wiki/Semiconductor.

[2] C. Sumbit, Ph.D. Thesis, Gauhati University India (2008) 52.

[3] K. Kano, "Semiconductor devices", Prentice-Hall, Inc. (1998) 39-40.

[4] S. K. Tewksbury, West Virginia University Morgantown., (1995) 3.

[5] W.S Lour, C.C. Chang, Solid State Electronics **39**; (1996)1295.

[6] F. Wagner, H. Wolf and Th. Wichert, and ISOLDE collaboration, Defect and Diffusion Forum **237** (2005) 491.

[7] G. F. Neumark, Mater. Sci. Eng. **21**, (1997) 1.

[8] L. D. Partain, Editor "Solar Cells and Their Applications", New York, Wiley (1995)

[9] R. W. Miles. Vaccum **80** (2006) 1090-1097.

[10] R. H. Bube "Photovoltaic Materials", Imperial College Press (1998)

[11] R.W. Miles, K.M. Hynes, I Forbes, Progress in Crystal Growth and char. Of mat., **51** (2005) 1-4.

[12] N.B. Chaure, J.P. Nair, R. Jayakrishan, V. Genesan, R.K. Pandey, Thin solid Films **324** (1998) 1443.

[13] E. A. Siebentritt S. L. Steiner M, Riedl W, Karg F. Sol Energy Mater Sol Cells **67** (2001) 31.

[14] B.Y. Oh,M.C. Jeong,T.H. Moon, W.M. Lee, J.M. Hwang, J.Y. Seo, D.Shik. Journal of Applied Physics **99** (2006) 12.

[15] F. Aglaa, I. Masaya, Sol. Energy Mater. Sol. Cells **747** (2005) 87.

[16] J.P. Enriquez, X. Mathew, Sol. Energy Mater. Sol. Cells **76** (2003) 313.

[17] B.M. Basol, S.S. Ou, and O.M Stafsudd, J. Appl. Phys. **58** (1985) 3809.

[18] Ma, C; Ding, Y; Moore, D; Wang, X; Wang, Zl Journal of the American Chemical Society **126** (2004) 708–9.

[19] S. Venkatachalam, D. Mangalaraj, Sa. K. Narayandass, K. Kim, J. Yi, J. Phys. D Appl. Phys **39** (2006) 4777-4782.

[20] M. C. Tamargo "II-VI Semiconductor Materials and their Applications", Taylor and Francis, New York, (2002).

[21] R. M. Park, M. B. Troffer, C. M. Rouleau, J. M. DePuydt and M. A. Haase, Appl. Phys. Lett. , **57** (1990) 2127-2129.

[22] Deutsch T F, J. Phys. Chem. Solids, 34 (1973) 2091.

[23] E. Masetti, M. Montecchi, and M. P. da Silva, Thin Solid Films, **234** (1993) 557.

[24] M. Bedir, M. Oztas, O. F. Bakkaloglu and R. Ormanci, Eur. Phys J. B",**45** (2005) 465-471.

[25] A. P. Samantilleke, I. M. Darmadasa, K. A. Prior, K. L. Choy, J. Mei, R. Bacewicz, A. Wolska, J. Mater. Sci. Mater. Electron, **12** (2001) 661-666.

[26] A. Nouhi, R. J. Stirn and A. Hermann, Proc. "19th IEEE Photovoltaic Specialistst Conf.", IEEE, New York, (1987) 1461.

[27] Y. Tsujimoto and M. Fukai, "Electoluminescence from ZnSe-ZnTe Heterojunction Diodes", Japan J. Appl. Phys., **6** (1967) 1024-1025.
[28] R. Markowski, M. Piacentinit, D. Debowskat, M. Zimnal-Starnawskat, F. Lamas, N ZemaJJ and A Kisielf, J. Phys.: Condens. Matter, **6** (1994) 3207-3219.
[29] J. Dutta, D Bhattacharyya, S. Chaudhuri, A.K. Pal, Sol. E. Mat. And Sol Cells **36** (1995) 357-368.
[30] F. I. Ezema, A.B.C. Ekwealor and R. u. Osuji, Turk J Phys, **30** (2006) 157-163.
[31] J. P. Enriquez, Z. Mathew, Sol. E. Mat. And Sol Cells, **76** (2003) 313-322.
[32] C.D. Lokhande, P.S. Patil, A. Ennaoui, H. Tributsch, App. Surface Sc., **123/124** (1998) 294-297.
[33] G.I. Rusu, et al J. Non-Crys. Solids **352** (2006) 1523-1528.
[34] G.I. Rusu, et al. App. Surface Sc., **253** (2007) 9500-9505.
[35] R. Chandarmohan, T. Mahalingam, J. P. Chu, P. J. Sebastian, Sol. E. Mat. And Sol Cells, **81** (2004) 371-378.
[36] S. Venkatachalam, D. Mangalaraj, Sa K. Narayandass, K. Kim, J Yi, Vaccum, **81** (2007) 928-933.
[37] S. Venkatachalam et al, Mat. Sc. in Semi. Processing, **10** (2007) 128-132.
[38] Zulfiqar Ali, A. K. S. Aqili, M Shafique, A. Maqsood, J. Non-Crys. Solids, **352** (2006) 409-414.
[39] A. K. S. Aqili, A. Maqsood, Zulfiqar Ali, App. Surface Sc., **191** (2002) 280-285.
[40] S.M. Sze, "Physics of Semiconductor Devices", 2nd ed. John Wiley & Sons, (1981) p.30-35
[41] D.K.Schroder, "Semiconductor material and device characterization", John Wiley& Sons, (1990) 2-34.
[42] J. P. Enriquez, Z. Mathew, Sol. E. Mat. And Sol Cells,, **76** (2003) 313
[43] L. Chen, D. Zhang, G. Zhai, J.Zhang, Materials Chemistry and Physics, **120** (2010) 456
[44] P.J. George, A. Sánchez-Juarez, P.K. Nair, Semicond. Sci. Tech. **11** (1996) 1.
[45] Rongbin Ye , Mamoru Baba,Koji Ohta, Kazunori Suzuki, **54** (2010) 710-714.